minerals

MDPI

Article

An Update on the Geochemical Composition of Peninsular India Rivers Average Clay (PIRAC): A Regional Reference for River Sediments of Peninsular India

Venigalla Purnachandra Rao [1,*], Shaik Sai Babu [2] and Mekala Ram Mohan [3]

[1] Department of Civil Engineering, Vignan's Foundation for Science, Technology and Research (VFSTR), Deemed to be Vignan's University, Vadlamudi, Guntur 522 213, Andhra Pradesh, India
[2] Department of Civil Engineering, K.S.R.M. College of Engineering, Kadapa 516 005, Andhra Pradesh, India; sksaibabu19932@gmail.com
[3] Council of Scientific and Industrial Research -National Geophysical Research Institute, Uppal Road, Hyderabad 500 007, Telangana, India; rammohan@ngri.res.in
* Correspondence: vprao55@gmail.com

Abstract

The rivers draining Peninsular India are rain-fed and their sediments are formed from weathering and erosion of continental rocks in the drainage basins. Peninsular India comprises dominantly the Archean–Proterozoic Terrain (APT) in the south, Deccan Trap Volcanic Terrain (DVT) in the middle, and Mixed-Lithology Terrain (MLT) in the north. Here, we highlight the differences in the average chemical composition of the clay fraction of sediments in rivers that drain dominantly similar geological terrains along the east and west coasts of India, update the geochemical composition of the Peninsular India Rivers Average Clay (PIRAC) based on the sediments from 104 rivers, and suggest that the composition of PIRAC serves as a regional reference for river sediments of Peninsular India. We found that the major elements in the clay fraction of sediments in the rivers are variably affected by the intensity of weathering. On an average, the clays from the east coast rivers showed higher Si, Ti, Fe, Mg, Mn and Na and lower Ca and P than those of the west coast. PIRAC showed more depleted Si, Mg, Ca, Na and K and enriched Ti, Fe, Mn and P relative to the Post-Archean average Australian Shale (PAAS). The clays were extremely weathered in southern Peninsular India, and strong to moderately weathered in central and northern Peninsular India. The average total trace element content (∑TE) of the clays was much higher for the east coast rivers than that of the west coast. The ∑TE of PIRAC was lower than in PAAS. The PAAS-normalised trace elements of PIRAC showed high transition trace elements, low high-field strength elements and large-ion lithophile elements. The average rare earth element content (∑REE) of the clays increased from APT to MLT for the east coast rivers but decreased in the west coast rivers. The ∑REE was lower for PIRAC than in PAAS. The PAAS-normalised REE of PIRAC showed MREE- and HREE-enriched and LREE-depleted pattern, with positive Ce and Eu anomalies. PIRAC is significantly enriched with mafic component dominated material despite Archean–Proterozoic rocks being abundantly widespread in Peninsular India. The intensity of chemical weathering, erosion and transportation of easily eroded mafic rocks relative to that of felsic rocks resulted in deposition of mafic component-dominated material at the lower reaches of almost all rivers. The composition of PIRAC is significantly different from other reference sediments. We suggest PIRAC serves as regional reference for river sediments of Peninsular India.

Check for updates

Academic Editor: Hermann Kudrass

Received: 31 July 2026
Revised: 17 September 2026
Accepted: 22 September 2026
Published: 25 September 2026

Copyright: © 2026 by the authors. Licensee MDPI, Basel, Switzerland. This article is an open access article distributed under the terms and conditions of the Creative Commons Attribution (CC BY) license.

Keywords: river sediments; clay; Peninsular India; felsic rocks; rare earth elements; weathering

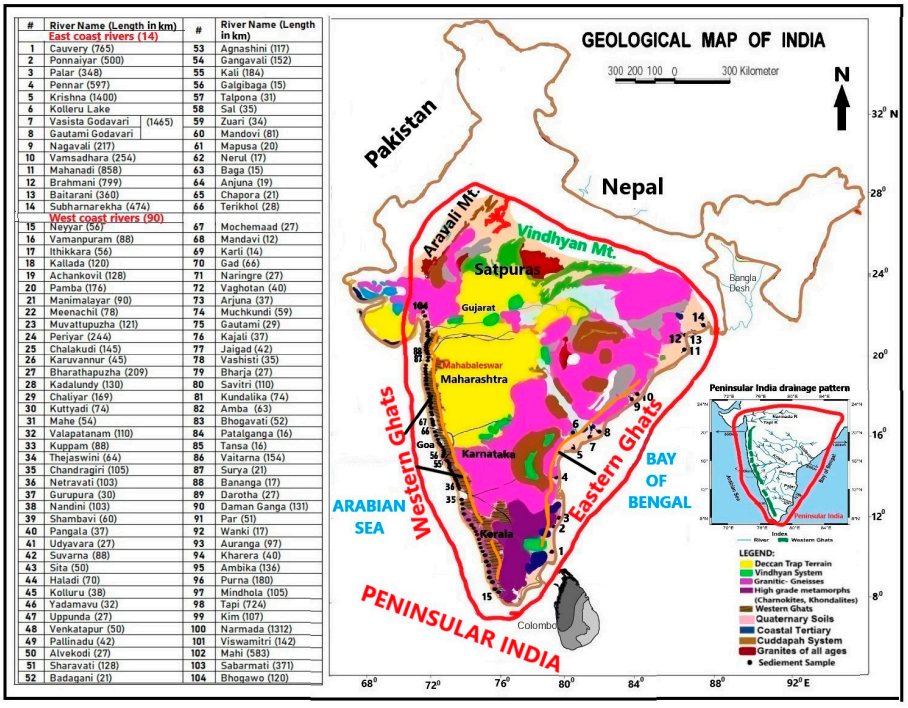
1. Introduction

Physiographic features, rivers and climate of Peninsular India

Peninsular India is an inverted triangular landmass, bound by the Western Ghats in the west, the Eastern Ghats (EG) in the east, the Aravali mountain ranges in the northwest, and Vindhyan and Satpura hill ranges in the northeast ([1]; Figure 1). Almost all rivers originate in mountain or hill ranges or high plateaus, drain continental rocks and flow westwards into the Arabian Sea, or eastwards into the Bay of Bengal. Although humid, tropical climate dominantly prevails over India, semi-arid conditions in the central and southcentral Peninsular India and arid conditions over its northwestern section have been reported [2]. The rivers receive abundant rainfall and runoff, especially during the monsoon months [3]. About 75% of India's total rainfall comes during the southwest monsoon (June–September) and the rest during the northeast monsoon (November to February). The average annual rainfall in India is ~1250 mm, but it has great spatial variations, as low as 500 mm in the central part of Peninsular India. The Western Ghats (WG) is a prominent geographic feature, stretching at ~1600 km along the west coast of India, with high relief and steep slope in its western flank and gentle slope in its eastern flank. It receives ~3000 mm annual rainfall. Numerous west-flowing rivers, originating from WG, are small and narrow, and transport their sediment-laden water into the Arabian Sea. Moreover, the Narmada and Tapti (major) Rivers originate from the Amarkantak plateau, and Satpura range, respectively, and flow westwards into the Arabian Sea. The Sabarmati River originates in the Aravalli range, while the Mahi River originates in the Vindhyan range, but both drain into the Arabian Sea. Several east-flowing rivers also originate in the western India. For example, the Cauvery, Krishna and Godavari (major) Rivers originate in the Western Ghats. The Ponnaiyar, Palar and Pennar Rivers originate in the west (Nandi hill ranges). The Mahanadi, Brahmani, Baitarani and Subarnarekha originate in the highlands or plateaus of Chhattisgarh. The Nagavali and Vamsadhara Rivers originate in the Eastern Ghats. Importantly, all these rivers drain different geological terrains, flow eastwards and bring their sediment load to the Bay of Bengal. The west- and east-flowing rivers account for ~23% and 77% of India's total drainage area, respectively. In other words, the drainage basins of the rivers cover almost the entire landmass of Peninsular India, approximately an area of 16,00,000 km^2 [1]. The average geochemical composition of sediments in the east- and west-flowing rivers should ideally serve as regional reference for river sediments of the Indian sub-continent.

The rivers draining Peninsular India are rain-fed and their sediments are formed from weathering and erosion of continental rocks in the drainage basins. The geochemistry of the sediments is affected by several factors, namely, source rocks, climate, topographic relief, intensity of physical and chemical weathering, loss to hydrosphere, element solubility, size sorting during transportation, and deposition and pollution [4–14]. Numerous studies have indicated that the major and trace element composition of the crustal sediments varies widely relative to that of reference sediments, Upper continental crust (UCC; [15,16]) and Post-Archean average Australian Shale (PAAS; [17,18]) and therefore does not reliably indicate crustal composition [19]. On the other hand, rare earth elements (REEs) are less fractionated and transferred near quantitatively into the sediments during erosion and sedimentation [20]. Therefore, it was thought that the average REE composition of the sediments is widely accepted to reflect the composition of the UCC and PAAS [21,22]. Subsequent studies, however, indicated REEs of the sediments are affected by several factors, including source rocks, grain size, mineralogy and heavy minerals [23–30]. Moreover, the REE composition of the sediments from certain environments can

deviate considerably from that of UCC and PAAS. By now, the geochemical compositions of reference sediments from different sub-continents and large rivers of the world are available. These include North American Shale Composite (NASC—[31]), European Shale (ES—[32]), Mud of Queensland (MUQ—[33]), East China Post-Archean Shale (ECPAS—[34]), composition of the Average Suspended Sediments of World Rivers (ASSWR—[35]) and REE composition of World River Average Clay (WRAC—[36]). Fine-grained sediments provide clues on the provenance and composition of the continental crust [5,37–39]. Keeping this in view, Babu et al. [29,40] published geochemical composition of the clay fraction (<4 μm size) of bottom sediments from 15 major and medium rivers and two lakes along the east coast of India. Of the 15 rivers, the Haldia and Hooghly are tributaries of the River Ganga (extra-Peninsular river) that bring sediments from glacial weathering of the Himalayas. The Chilika Lake is brackish water lake. Babu et al. [41] excluded the geochemistry of sediments from Haldia and Hooghly rivers and Chilika Lake, and reported the composition of Peninsular India rivers average clay for the Indian sub-continent, based on the sediments from 14 rivers (including sediment from Kolleru (fresh water) Lake, considered as river sediment) [41]. Several others [42–45] also published papers on the geochemistry of river sediments. Numerous rivers drain the western margin of India and discharge their sediment load into Arabian Sea, and there is a lack of coherent geochemical data on bottom sediments from these rivers. Recently, Babu et al. [30,46–48] reported geochemical composition of the clay fraction (<4 μm size) of bottom sediments from 90 rivers along the west coast of India. There is a need to integrate the geochemical data of the bottom sediments in rivers along the east and west coasts of India. In this paper, we used the geochemical data set of Babu et al. [29,30,40,46–48] to (a) highlight the differences in the geochemical composition of the clay fraction of bottom sediments in the rivers that drain similar geological terrains along the east and west coasts of India, (b) update the geochemical composition of Peninsular India Rivers Average Clay (PIRAC) based on the clay fraction of sediments from 104 rivers, and (c) suggest that the composition of PIRAC serves as a regional reference for river sediments of Peninsular India.



#	River Name (Length in km)	#	River Name (Length in km)
	East coast rivers (14)		
1	Cauvery (765)	53	Agnashini (117)
2	Ponnaiyar (500)	54	Gangavali (152)
3	Palar (348)	55	Kali (184)
4	Pennar (597)	56	Galgibaga (15)
5	Krishna (1400)	57	Talpona (31)
6	Kolleru Lake	58	Sal (35)
7	Vasista Godavari (1465)	59	Zuari (34)
8	Gautami Godavari	60	Mandovi (81)
9	Nagavali (217)	61	Mapusa (20)
10	Vamsadhara (254)	62	Nerul (17)
11	Mahanadi (858)	63	Baga (15)
12	Brahmani (799)	64	Anjuna (19)
13	Baitarani (360)	65	Chapora (21)
14	Subharnarekha (474)	66	Terikhol (28)
	West coast rivers (90)		
15	Neyyar (56)	67	Mochemaad (27)
16	Vamanpuram (88)	68	Mandavi (12)
17	Ithikkara (56)	69	Karli (14)
18	Kallada (120)	70	Gad (66)
19	Achankovil (128)	71	Naringre (27)
20	Pamba (176)	72	Vaghotan (40)
21	Manimalayar (90)	73	Arjuna (37)
22	Meenachil (78)	74	Muchkundi (59)
23	Muvattupuzha (121)	75	Gautami (29)
24	Periyar (244)	76	Kajali (37)
25	Chalakudi (145)	77	Jaigad (42)
26	Karuvannur (45)	78	Vashisti (35)
27	Bharathapuzha (209)	79	Bharja (27)
28	Kadalundy (130)	80	Savitri (110)
29	Chaliyar (169)	81	Kundalika (74)
30	Kuttyadi (74)	82	Amba (63)
31	Mahe (54)	83	Bhogavati (52)
32	Valapatanam (110)	84	Patalganga (16)
33	Kuppam (88)	85	Tansa (16)
34	Thejaswini (64)	86	Vaitarna (154)
35	Chandragiri (105)	87	Surya (21)
36	Netravati (103)	88	Bananga (17)
37	Gurupura (30)	89	Darotha (27)
38	Nandini (103)	90	Daman Ganga (131)
39	Shambavi (60)	91	Par (51)
40	Pangala (37)	92	Wanki (17)
41	Udyavara (27)	93	Auranga (97)
42	Suvarna (88)	94	Kharera (40)
43	Sita (50)	95	Ambika (136)
44	Haladi (70)	96	Purna (180)
45	Kolluru (38)	97	Mindhola (105)
46	Yadamavu (32)	98	Tapi (724)
47	Uppunda (27)	99	Kim (107)
48	Venkatapur (50)	100	Narmada (1312)
49	Pallinadu (42)	101	Viswamitri (142)
50	Alvekodi (27)	102	Mahi (583)
51	Sharavati (128)	103	Sabarmati (371)
52	Badagani (21)	104	Bhogawo (120)

Figure 1. The geological map of India. The area bound by red line denotes Peninsular India. Sediment sample locations in the rivers are indicated by dots (with numbers) along the east and west coast of India. The name of the river is also given. Physiographic features surrounding Peninsular India are also shown. Insert map shows the drainage network of the rivers in Peninsular India (modified after GSI, [49]).

2. Geology of the Drainage Basins

Peninsular India comprises three dominant lithological terrains latitudinally: the Archean–Proterozoic Terrain (APT) in the south, Deccan Trap Volcanic Terrain (DVT) followed by Archean–Proterozoic rocks in the centre, and Mixed-Lithology Terrain (MLT) in the north (Figure 1). The Archean–Proterozoic Terrain (APT) comprises the Archean (pyroxene granulites and biotite-hornblende gneisses, granodiorite, diorite, and pegmatites, principally granitic intrusives into metamorphic schists) and Precambrian (granites, charnockites, and gneisses) rocks [50]. The drainage basins comprise TTG-type Peninsular gneiss, dioritic to tonalite gneiss and their granulite grade charnockite, granite and minor amounts of Archean supra-crustal rocks [42]. A thick lateritic cover occurs on basement rocks. The Nagavali and Vamsadhara Rivers drain the Precambrian khondalite (garnet-sillimanite gneiss) of the Eastern Ghats mobile belt. The Godavari and Krishna, central Peninsular India rivers, largely drain through Deccan Trap Volcanic Terrain (DVT) in the upper reaches, followed by Archean granites and gneisses, Precambrian charnockite/khondalite rocks, and deltaic sediments in the middle and lower reaches [51,52]. The Mixed-Lithology Terrain (MLT) in the north consists of igneous rocks and Late Archaean ore deposits of oxides and sulfides (Singhbhum formations) in the upper reaches, lateritic, yellow, and red soils and deltaic soils in the lower reaches [53]. Precambrian rocks (granites, gneisses, khondalites) and sedimentary sequences ranging from Cretaceous to Holocene are also present in the drainage area. The Mahanadi, Brahmani and Subarnarekha Rivers drain through MLT. The lower basin of the Brahmani River also receives contributions from high-grade metamorphic rocks of the Eastern Ghats Mobile Belt and younger Gondwana sedimentary formations. Consequently, the Brahmani sediments integrate material derived from Archean granitoids, banded iron formations, metasedimentary rocks, and recycled sedimentary units [54]. Bhattacharya et al. [55] reported high ilmenite, rutile, zirconium, and rare earth minerals in its drainage basin. Indeed, the west-flowing rivers along western India drain similar geological terrains but transport their sediment loads into the Arabian Sea. One should note that the east-flowing rivers are major and medium rivers, draining source rocks on a gentle slope. They experience various climatic zones and their sediments have long transportation and reworking histories, whereas the west-flowing rivers are minor and medium rivers (except Narmada and Tapti), experience heavy rainfall and drain a few rock types exhibiting high relief and steep slope, and their sediments are expected to represent weathering environment typical of their basins. Here, we have compiled the geochemical composition of the clay fraction (<4 μm) of sediments deposited at the lower reaches of 104 rivers, and compared the differences in the geochemical composition of sediments in rivers that drain similar geological terrains along the east and west coasts of India.

3. Materials and Methods

Bottom sediments were collected at the lower reaches (10–30 km away from the high tide levels in the rivers) of 14 rivers along the east coast of India and 90 rivers along the west coast of India (Figure 1). One sample was collected at mid-stream from each river during April–May, using a Peterson Grab and mechanised boat. We presume that there is no seasonal effect on bottom sediments, as monsoonal hydrodynamics start during the SW monsoon (June–September) and NE monsoon (November–February). The top portion of the sediments was preserved in polythene bags, numbered and brought to the laboratory. Part of the sample was taken in a 500 mL glass beaker and dried in an oven at 60 °C. Following Folk [56], the sand (>62 μm), silt (>4 to <62 μm), and clay (<4 μm) fractions of the total sediment were separated and dried. The geochemical composition of the clay (<4 μm) fraction was determined, following standard procedures detailed in

Babu et al. [29,30,40,41,46–48]. Ten major elements (Si, Al, Fe, Mg, Mn, Ti, Ca, Na, K, P) were determined with X-ray fluorescence spectrometer, 'WD-XRF' Model Axios mAX, PAN-analytical, using JSd-1 as the standard, at the CSIR–National Geophysical Research Institute (CSIR-NGRI), Hyderabad. For trace elements, closed acid digestion, using HF:HNO_3 is adopted. Detailed procedure for the preparation of sample solutions for trace elements was given in Babu et al. [40]. Trace elements were analysed by High-Resolution Inductively Coupled Plasma Mass Spectrometer (HR-ICP MS), Nu Instruments, UK at CSIR-NGRI. Nineteen trace elements (Sc, V, Cr, Co, Ni, Cu, Zn, Pb, Ga, Rb, Sr, Nb, Cs, Ba, Zr, Hf, Th, U, and Ta) and fifteen rare earth elements (La, Ce, Pr, Nd, Sm, Eu, Gd, Tb, Dy, Y, Ho, Er, Tm, Yb, Lu) were analysed. MAG-1 (marine mud), certified reference material (CRM) from the United States Geological Survey, was used as calibrating standard for the analysis of sediments, and JSd-1, CRM for stream sediments from the Geological Survey of Japan, was used as a cross-check standard for the data. Rh^{103} was used as an internal standard for instrument drift correction. The drainage basins of the rivers cover the entire landmass of Peninsular India, measuring an area of approximately 16,00,000 km^2 [1]. The geochemical data of sediment samples collected at the lower reaches of 104 rivers along the east and west coast of India were published in different papers [29,30,40,41,46–48]. In this paper, we have systematically brought out the differences in average geochemical composition of the sediments in rivers draining similar geological terrains along the east and west coasts of India. The average geochemical composition of the clay fraction of sediments from all rivers, referred to here as Peninsular India Rivers Average Clay (PIRAC) was calculated and compared the geochemical composition of PIRAC with other reference sediments. We believe that the geochemical composition of PIRAC would serve as a regional reference for river sediments of Peninsular India.

4. Results

4.1. Distribution of Major Elements

Table 1 shows the major element data in the clay fraction of river sediments draining APT, DVT and MLT. Figure 2 shows the PAAS-normalised average distribution of major elements in the clays from each terrain, in the clays from the rivers of the east and west coast of India and in the clays from all rivers (PIRAC). In general, mobile elements (Si, Ca, Mg and K) were depleted and immobile elements (Al, Fe, Ti and P) enriched, relative to that of PAAS in every terrain. Relatively high SiO_2, Al_2O_3, Fe_2O_3, MnO, MgO, Na_2O and K_2O and low TiO_2, CaO and P_2O_5 were characteristic of the clays from the east coast rivers compared to that of west coast rivers (Figure 2). The PAAS-normalised PIRAC showed depleted Si, Ca and K, enriched Ti, Fe, Mn, Mg, Na and P and similar Al content. The UCC-normalised PIRAC showed enriched Ti, Al, Fe, Mn and P and depleted Si, Ca, MG, Na and K (Figure 2). The average SiO_2/Al_2O_3 of the clays for APT, DVT and MLT was 1.95, 2.54 and 3.29, respectively for the west coast rivers, and 2.72, 3.06 and 2.69 for the east coast rivers. The SiO_2/Al_2O_3 was significantly low for PIRAC (2.29) compared to UCC (4.33) and PAAS (3.32). The average TiO_2 content was high in DVT, followed by MLT and lowest in APT clays (Table 1). The average Al_2O_3/TiO_2 was high for APT (18.59) and significantly low for DVT (12.35) and MLT (12.37). The Al_2O_3/TiO_2 was much lower for PIRAC (14.61) than in UCC (24.29) and PAAS (18.9).

The Chemical Index of Alteration (CIA) is used to measure the intensity of weathering [57]. The average CIA values of the clays ranged from 69.5 to 86.7 for the east coast rivers and from 61.78 to 96.6 for the west coast rivers. The ternary diagram A-CN-K ($Al_2O_3 - (CaO + Na_2O) - K_2O$) integrated with CIA values (Figure 3A) shows that the clays from the west coast rivers followed a systematic shift from APT to MLT, with APT samples plotting close to apex A, DVT samples plotting slightly away from apex A, and

MLT samples plotting much away from apex A and on either side of the line separating strong and intermediate weathering. The clays from the east coast rivers showed strong weathering for APT and strong to intermediate weathering for DVT and MLT. The clays from all rivers (PIRAC) showed samples plotting almost parallel to A-CN axis, extending from intermediate weathering to strong weathering. CIA showed positive correlation with Al_2O_3 and TiO_2 and negative correlation with FeO, MgO, K_2O and CaO (Figure 4).

The Plagioclase Index of Alteration (PIA) highlights the depletion of plagioclase, which typically weathers more rapidly than K-feldspar. It is used to quantify the degree of weathering of plagioclase feldspar [58–62]. The PIA values extend from 68 to 94 for the clays from west coast rivers and from 75 to 90 for the clays from east coast rivers (Table 1). The ternary diagram ((A-K)-C-N), ($(Al_2O_3–K_2O)$-CaO–Na_2O) integrated with PIA values (Figure 3B) showed a systematic decrease from APT to DVT and then to MLT for the west coast rivers and value plot parallel to C-(A-K) axis. For the east coast rivers, high PIA values correspond to APT and MLT and low values to DVT. PIA values plot parallel to the N-(A-K) axis (Figure 3B).

The A-CNK-FM diagram is used to evaluate the weathering trends, and position of the sample on the plot reveals geological history during weathering [63,64]. Virtually all samples plot away from apex CNK in this diagram (Figure 3C). The clays from the west coast rivers, especially from APT and DVT, plot parallel to A-FM line and more towards apex A. The clays from MLT plot slightly away from A-FM line and more towards PAAS value (Figure 3C). The clays from east coast rivers plot slightly away from A-FM line and more towards PAAS value (Figure 3C).

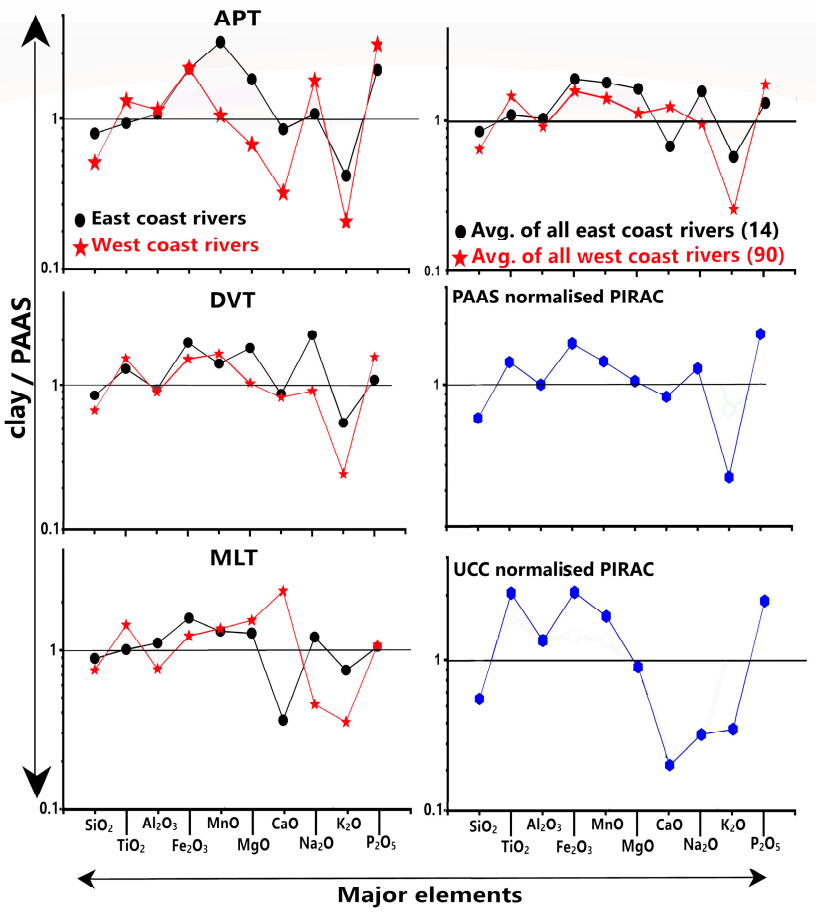


Figure 2. PAAS-normalised average major element distribution in the clays from each terrain, in the clays from the rivers of the east and coast of India, and in the clays of all rivers (PIRAC). UCC normalised PIRAC is also shown.

Table 1. Major element content (%) of the clay (<4 μm) fraction of sediments in the rivers of the east coast and west coast of India.

		SiO_2	Al_2O_3	Fe_2O_3	FeO	MnO	CaO	MgO	K_2O	Na_2O	TiO_2	P_2O_5	SiO_2/Al_2O_3	Al_2O_3/TiO_2	CIA	PIA	ICV
East coast rivers draining APT (6)	Range	52.35–55.96	17.68–22.95	11.46–13.07	10.31–11.76	0.11–0.58	0.36–1.91	2.29–4.39	1.59–2.51	0.64–1.80	0.72–1.72	0.18–0.55	2.32–3.17	10.82–31.74	77.10–86.73	83.02–94.26	0.83–1.30
	Avg.	53.42	19.82	12.24	11.01	0.25	1.16	3.34	2.01	1.26	0.95	0.27	2.72	22.85	81.59	87.90	1.09
	STD (±)	1.32	2.21	0.60	0.54	0.18	0.70	0.98	0.41	0.45	0.38	0.14	0.32	7.04	3.46	4.27	0.20
West coast rivers draining APT (52)	Range	29.01–52.33	11.37–32.01	6.32–17.71	5.69–15.94	0.02–0.58	0.11–2.96	0.29–3.87	0.51–2.88	0.06–25.28	0.71–1.97	0.10–0.83	1.05–2.91	9.23–37.04	79.64–96.60	73.35–94.35	0.44–3.76
	Avg.	38.89	20.82	12.34	11.10	0.11	0.59	1.65	1.21	1.80	1.21	0.35	1.95	18.10	86.85	81.81	0.98
	STD (±)	5.11	3.82	2.42	2.18	0.10	0.44	0.85	0.44	4.79	0.27	0.15	0.47	5.77	13.17	13.95	0.55
APT (58)	**Range**	**29.01–55.96**	**11.37–32.01**	**6.32–17.71**	**5.69–15.94**	**0.02–0.58**	**0.11–2.96**	**0.29–4.39**	**0.51–2.88**	**0.06–25.28**	**0.71–1.97**	**0.10–0.83**	**1.05–3.17**	**9.23–37.04**	**77.10–96.60**	**73.35–94.35**	**0.44–3.76**
	Avg.	**40.39**	**20.71**	**12.33**	**11.09**	**0.13**	**0.65**	**1.83**	**1.29**	**1.75**	**1.18**	**0.34**	**2.03**	**18.59**	**86.30**	**82.44**	**0.99**
	STD (±)	**6.59**	**3.68**	**2.30**	**2.07**	**0.11**	**0.49**	**1.00**	**0.50**	**4.54**	**0.29**	**0.15**	**0.52**	**6.02**	**12.61**	**13.39**	**0.53**
East coast rivers draining DVT (4)	Range	51.70–54.56	15.81–22.16	12.21–14.55	10.99–13.09	0.13–0.19	0.98–1.46	2.69–4.39	1.91–2.24	0.51–3.55	1.12–1.58	0.12–0.23	2.33–3.45	10.89–19.76	69.58–81.49	73.52–90.23	1.10–1.78
	Avg.	53.15	17.75	13.85	12.46	0.15	1.13	3.90	2.05	2.59	1.28	0.17	3.06	14.26	75.54	81.19	1.43
	STD (±)	19.95	9.79	5.75	5.18	0.01	0.11	0.53	0.48	1.69	0.52	0.11	0.88	7.33	42.39	39.70	0.26
West coast rivers draining DVT (21)	Range	28.32–51.21	13.71–21.65	3.13–14.67	2.82–13.20	0.07–0.44	0.26–2.10	0.79–5.72	0.55–1.34	0.12–13.22	0.63–2.98	0.06–0.54	1.87–3.32	7.27–29.27	78.14–94.06	72.31–91.36	0.42–2.13
	Avg.	42.28	16.90	10.75	9.67	0.18	1.07	2.23	0.91	1.09	1.51	0.25	2.54	11.98	85.19	80.59	1.08
	STD (±)	4.74	2.28	2.51	2.26	0.10	0.53	1.20	0.29	2.79	0.44	0.10	0.42	4.33	9.25	9.28	0.34
DVT (25)	**Range**	**28.32–54.56**	**13.71–22.16**	**3.13–14.67**	**2.82–13.20**	**0.07–0.44**	**0.26–2.10**	**0.79–5.72**	**0.55–2.24**	**0.12–13.22**	**0.63–2.98**	**0.06–0.54**	**1.87–3.45**	**7.27–29.27**	**69.58–94.06**	**72.31–91.36**	**0.42–2.13**
	Avg.	**44.01**	**17.03**	**11.24**	**10.12**	**0.17**	**1.08**	**2.50**	**1.09**	**1.33**	**1.48**	**0.23**	**2.62**	**12.35**	**83.64**	**80.69**	**1.14**
	STD (±)	**5.97**	**2.36**	**2.60**	**2.34**	**0.09**	**0.49**	**1.33**	**0.50**	**2.66**	**0.42**	**0.10**	**0.46**	**4.27**	**9.37**	**8.83**	**0.35**
East coast rivers draining MLT (4)	Range	53.19–58.21	20.10–22.18	10.6–12.24	9.61–11.01	0.07–0.18	0.36–0.62	2.32–3.37	2.47–3.24	0.61–2.10	0.93–1.09	0.16–0.17	2.39–2.89	18.36–22.45	79.04–84.56	86.78–94.73	0.89–1.03
	Avg.	56.16	20.93	11.47	10.32	0.15	0.47	2.82	2.79	1.46	1.01	0.17	2.69	20.77	81.56	90.52	0.96
	STD (±)	2.13	0.89	0.66	0.60	0.05	0.12	0.46	0.32	0.62	0.08	0.01	0.21	1.75	2.83	3.31	0.07
West coast rivers draining MLT (17)	Range	42.88–50.36	13.04–16.24	6.13–10.57	5.52–9.51	0.10–0.24	1.65–6.38	2.51–4.29	0.66–1.83	0.18–1.31	0.99–2.20	0.11–0.36	2.71–3.77	7.38–16.10	69.91–84.18	62.26–80.77	0.88–1.65
	Avg.	47.35	14.43	8.91	8.02	0.15	3.05	3.39	1.29	0.54	1.44	0.17	3.29	10.39	75.01	68.39	1.31
	STD (±)	2.50	0.86	1.10	0.99	0.03	1.06	0.49	0.38	0.36	0.29	0.07	0.29	2.06	5.43	6.70	0.17
MLT (21)	**Range**	**42.88–58.21**	**13.04–22.18**	**6.13–12.24**	**5.52–11.01**	**0.07–0.24**	**0.36–6.38**	**2.32–4.29**	**0.66–3.24**	**0.18–2.10**	**0.93–2.20**	**0.11–0.36**	**2.39–3.77**	**7.38–22.45**	**69.91–84.56**	**62.26–94.73**	**0.88–1.65**
	Avg.	**49.03**	**15.67**	**9.40**	**8.45**	**0.15**	**2.56**	**3.28**	**1.58**	**0.71**	**1.36**	**0.17**	**3.18**	**12.37**	**76.26**	**72.60**	**1.24**
	STD (±)	**4.27**	**2.75**	**1.45**	**1.30**	**0.03**	**1.41**	**0.52**	**0.70**	**0.55**	**0.31**	**0.07**	**0.37**	**4.62**	**5.63**	**10.81**	**0.20**

Table 1. *Cont.*

	Over all range	28.32–58.21	11.37–32.01	3.13–17.71	2.82–15.94	0.02–0.58	0.11–6.38	0.29–5.72	0.51–3.24	0.06–25.28	0.63–2.98	0.06–0.83	1.05–3.77	7.27–37.04	69.58–96.60	62.26–94.73	0.42–3.76
PIRAC (104)	**Over all avg.**	**43.01**	**18.81**	**11.48**	**10.33**	**0.14**	**1.14**	**2.28**	**1.30**	**1.44**	**1.29**	**0.28**	**2.29**	**14.61**	**83.64**	**80.03**	**1.07**
	Over all STD (±)	1.20	0.68	0.60	0.54	0.04	0.53	0.40	0.12	2.00	0.07	0.04	0.08	0.93	3.49	2.29	0.16
Reference Sediments	**UCC**	**66.20**	**15.30**	**5.57**	**5.01**	**0.09**	**3.57**	**2.47**	**2.78**	**3.25**	**0.63**	**0.15**	**4.33**	**24.29**	**61.44**	**50.28**	**1.20**
	PAAS	**62.80**	**18.90**	**7.22**	**6.50**	**0.11**	**1.30**	**2.20**	**3.70**	**1.20**	**1.00**	**0.16**	**3.32**	**18.90**	**75.29**	**60.56**	**0.89**

CIA: Chemical Index of Alteration [58]; PIA: Plagioclase Index of Alteration [59]; ICV: Index of Chemical Variability [6,65]; APT: Archean–Proterozoic Terrain (this study); DVT: Deccan Trap Volcanic Terrain (this study); MLT: Mixed-Lithology Terrain (this study); PIRAC: Peninsular India Rivers Average Clay (this study); UCC: Upper Continental Crust [16]; PAAS: Post-Archean average Australian Shale [18].

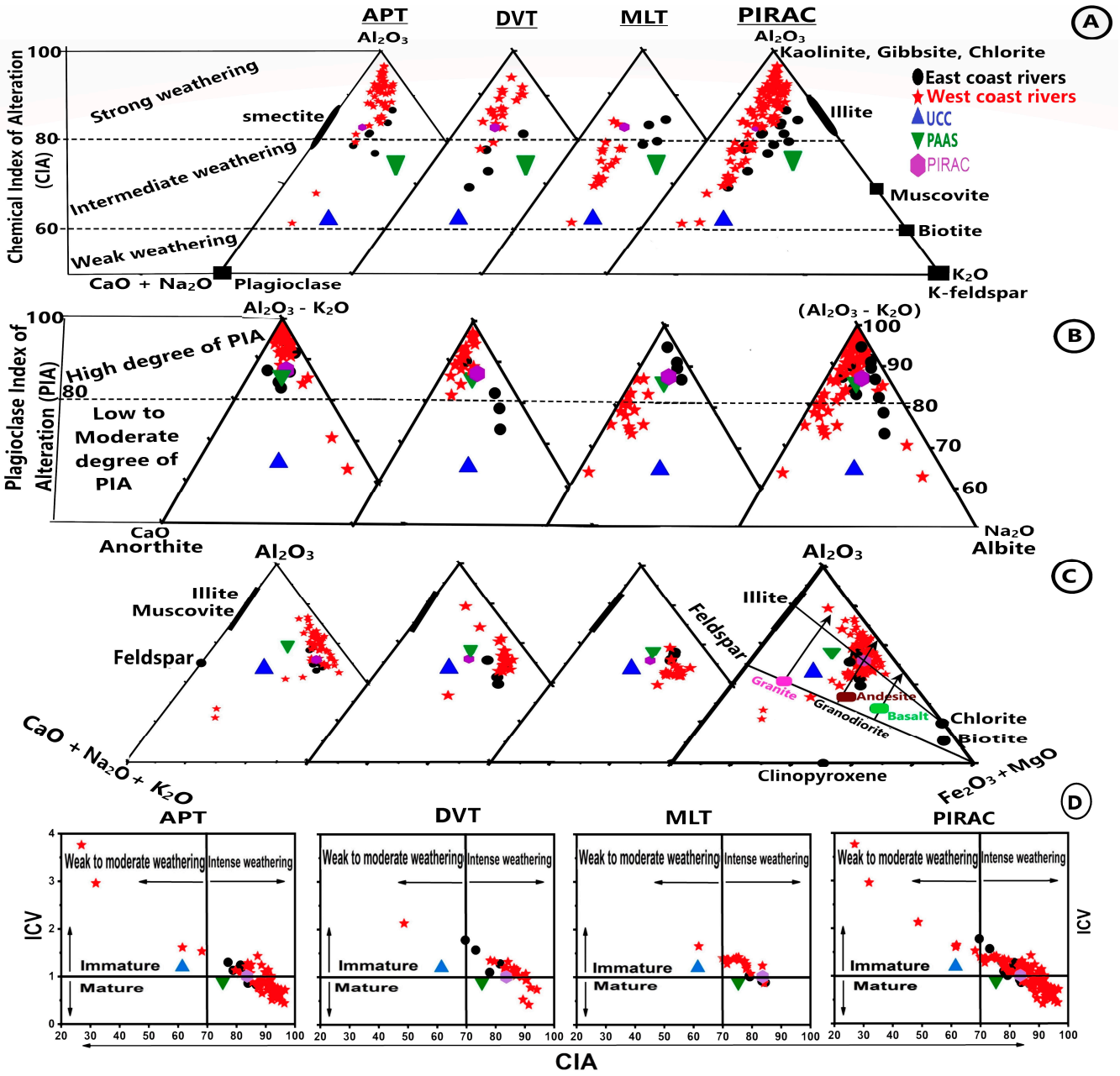


Figure 3. Ternary weathering diagrams showing: (**A**) the Chemical Index of Alteration, calculated as CIA = [Al_2O_3/(Al_2O_3 + CaO* + Na_2O + K_2O)] × 100 [58]; (**B**) the Plagioclase Index of Alteration, calculated as PIA = [(Al_2O_3 − K_2O)/(Al_2O_3 + CaO* + Na_2O − K_2O)] × 100 [59]; (**C**) the A–CNK–FM diagram [Al_2O_3 − (CaO + Na_2O + K_2O) − (Fe_2O_3 + MgO)] [63,64]; and (**D**) the relationship between the Chemical Index of Alteration (CIA) and the Index of Chemical Variability, where ICV = (Fe_2O_3 + K_2O + Na_2O + CaO + MgO + MnO + TiO_2)/Al_2O_3 [6].

The Index of Chemical Variability (ICV) evaluates the maturity of sediments. The ICV values > 1 indicate immature sediments, and values < 1 indicate mature sediments [6]. The average ICV values were 0.98, 1.08 and 1.31 for APT, DVT and MLT, respectively for the clays from west coast rivers, and 1.09, 1.43 and 0.96 for the east coast rivers (Table 1). The ICV values are ~1 for the clays from APT and DVT of the west coast, and APT and MLT of the east coast, indicating mature sediments. Figure 3D shows the plot of ICV values against CIA, indicating the inverse relationship between maturity and weathering intensity in the sediments from all terrains. We realise that the ICV values are also affected by the dominance of mafic component in the sediments. The average high ICV value (1.43) coincides with high abundance of Fe_2O_3

+ MgO (av. 17.75%; Table 1) in DVT sediments of the east coast, suggesting that the high ICV is due to the dominance of mafic component, rather than immaturity. The MLT sediments of the west coast plot in the region of intense weathering and immaturity (Figure 3D). However, the average high ICV (1.31) coincides with an average Fe_2O_3 + MgO of 12.30% (Table 1). Since arid climatic conditions are prevalent in the northwest India, it is likely that the high ICV values are due to the combined influence of mafic component and sediments derived from arid climatic conditions.

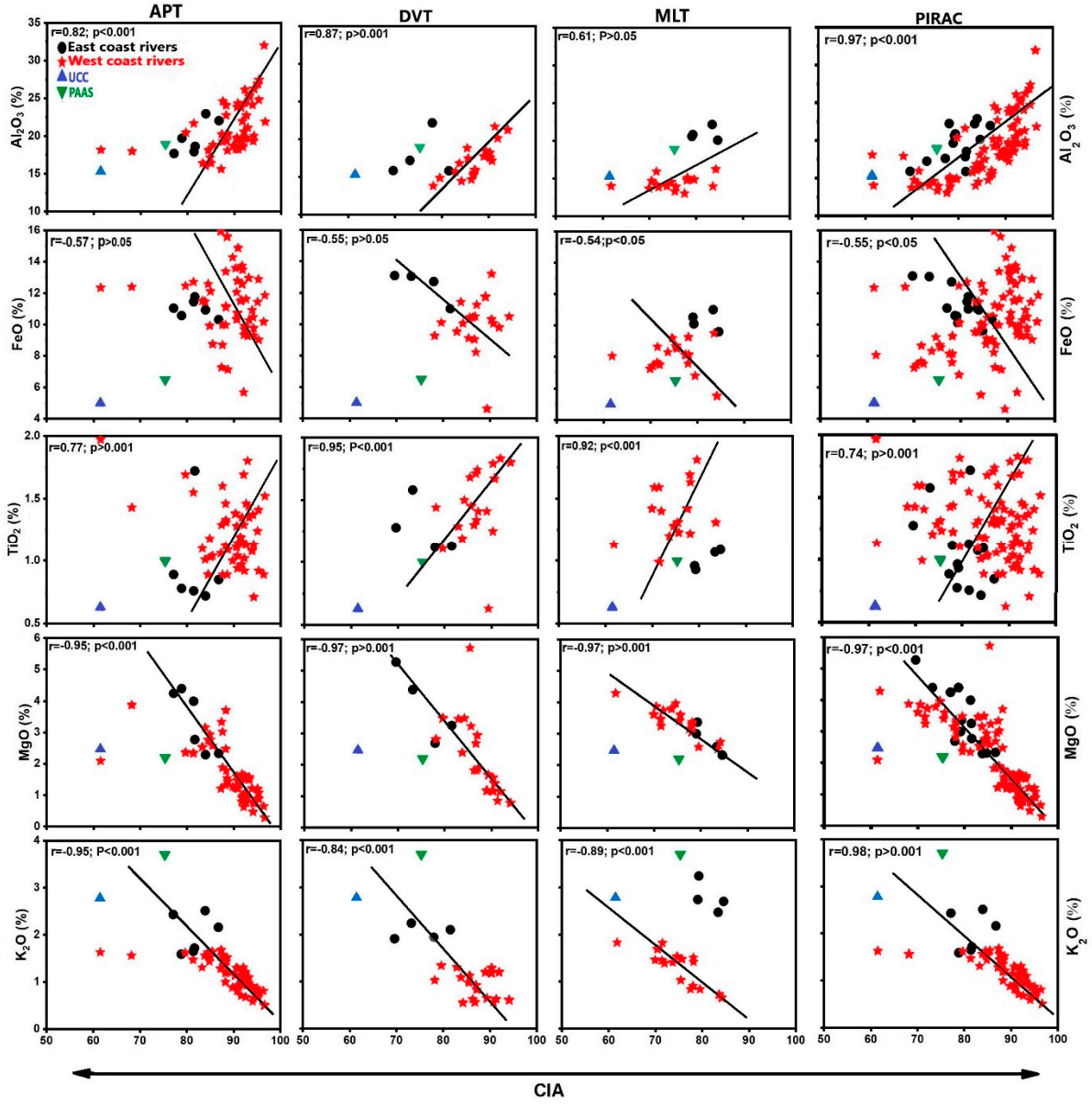


Figure 4. Correlation plots showing the relationships between CIA and Al_2O_3, FeO, TiO_2, MgO, and K_2O.

4.2. Distribution of Trace Elements

Table 2 shows trace element (TE) data in the clay fraction of sediments in rivers draining APT, DVT and MLT. The average total trace element content (∑TE) was high for APT (2203 µg/g), decreased to 1626 µg/g for DVT and then to 1318 µg/g for MLT for the east coast river clays. It was highest for DVT (1625 µg/g) followed by MLT (1597 µg/g and least for APT (1370 µg/g) clays for the west coast rivers, (Table 2). The average ∑TE of clays from all rivers (PIRAC: 1515 µg/g) was much lower than in UCC (1650.87 µg/g)

and PAAS (1807.1 µg/g). Figure 5 shows the PAAS-normalised average trace element (TE) distribution in the clays from each terrain, in the clays from the east coast and west coast rivers and in the clays from all rivers (PIRAC). It showed enriched transition trace element (TTE), slightly depleted high-field strength elements (HFSE) and much depleted large-ion lithophile elements (LILE) for the clays from all terrains of the west coast rivers. The average trace elements distribution was at variance for the clays from the east coast rivers (Figure 5). Among TTE, Cu, Zn and Pb contents were much higher and Sc, V, Cr, Co and Ni were either close to, or slightly enriched relative to PAAS. Among HFSE, Zr, Hf, Ta and Nb were much depleted and Th, Ga and U were slightly depleted or close to PAAS. LILE (Rb, Sr, Ba, Cs) were much lower than in PAAS in all terrains. The PAAS-normalised trace elements distribution of PIRAC (Figure 5) showed enriched TTE, slightly depleted HFSE and much depleted LILE. The UCC-normalised PIRAC showed enriched TTE, and HFSE and LILE close to UCC (Figure 5).

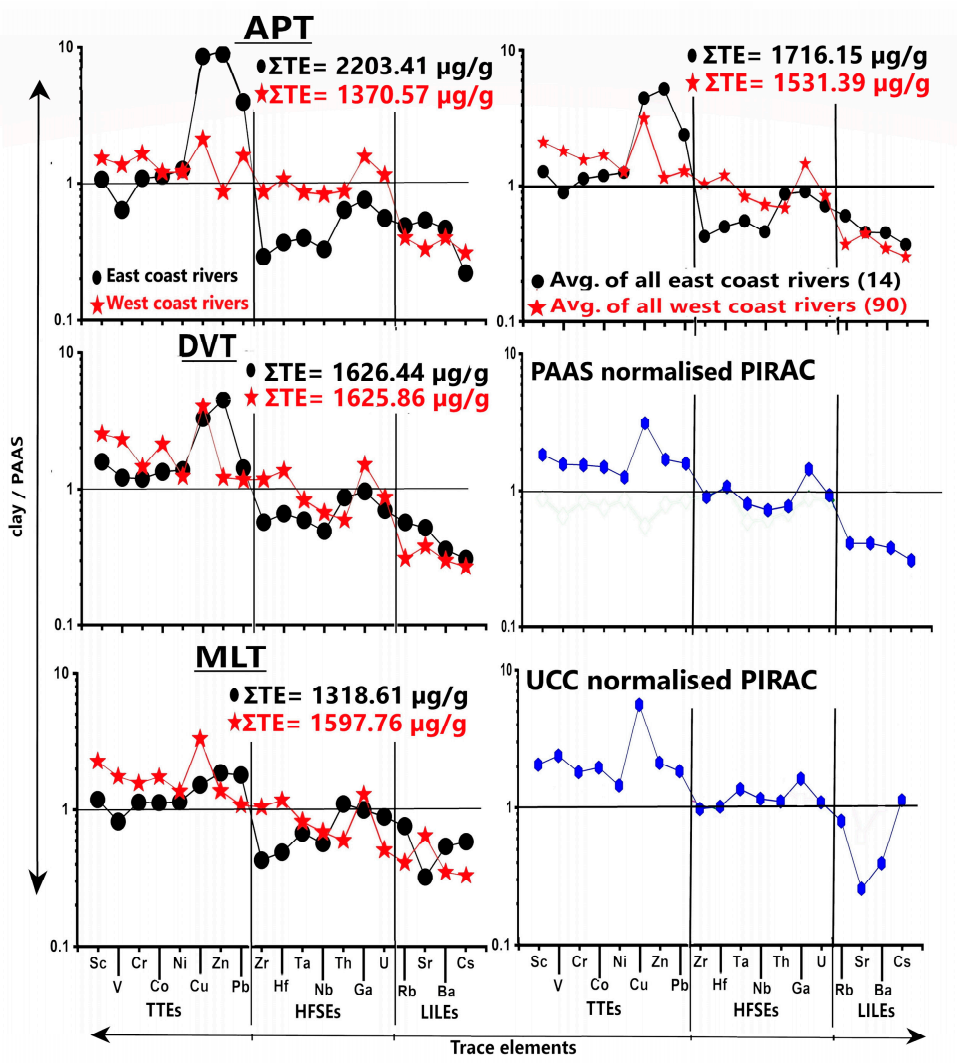


Figure 5. PAAS-normalised average trace element (TE) distribution in the clays from each terrain, in the clays from the rivers of the east and coast of India and in the clays of all rivers (PIRAC). UCC normalised PIRAC is also shown.

Table 2. Trace element content (μg/g) of the clay fraction (<4 μm) of sediments in the rivers of the east coast and west coast of India.

Rivers		Sc	V	Cr	Co	Ni	Cu	Zn	Pb	∑TTE	Zr	Hf	Ta	Nb	Th	Ga	U	∑HFSE	Rb	Sr	Ba	Cs	∑LILE	∑TE
East coast rivers draining APT (6)	Range	12.85–23.79	71.72–119.76	100.03–168.92	19.28–38.89	1.87–84.93	137.37–1068.14	274.03–1519.56	38.34–163.19	**803.74–3003.92**	45.16–102.34	1.37–2.97	0.45–0.94	4.76–9.02	6.25–16.04	11.87–18.30	1.34–2.75	**73.30–151.62**	47.69–124.64	68.41–172.29	189.59–439.51	1.51–6.41	**344.65–595.68**	**1494.10–3542.98**
	Avg.	16.96	96.37	119.49	25.98	69.68	429.06	776.62	79.89	**1614.06**	60.60	1.83	0.61	6.25	9.36	15.22	1.74	**95.60**	78.61	108.57	303.30	3.28	**493.75**	**2203.41**
	STD (±)	4.66	16.14	25.08	6.74	8.85	355.00	466.29	52.80	**797.87**	21.47	0.58	0.18	1.57	3.62	3.01	0.53	**29.79**	32.91	37.91	89.50	2.01	**84.57**	**747.30**
West coast rivers draining APT (52)	Range	14.31–36.60	111.23–347.62	82.78–897.43	11.40–55.13	42.60–129.46	29.21–231.78	29.81–195.44	12.15–88.87	**459.84–1605.29**	106.62–393.67	3.65–10.59	0.74–2.39	11–26.54	7.10–25.70	23.87–39.11	1.54–7.62	**175.31–474.78**	31.91–91.32	29.47–160.75	104.13–805.44	2.40–7.33	**168.83–1030.55**	**991.58–2027.72**
	Avg.	24.47	205.86	182.28	27.88	66.90	106.50	74.21	32.27	**720.37**	182.54	5.39	1.29	15.72	12.82	31.75	3.59	**253.10**	64.44	65.91	261.40	4.61	**396.36**	**1370.57**
	STD (±)	5.37	55.03	110.18	9.50	15.70	45.14	31.88	12.63	**184.95**	56.01	1.35	0.38	3.18	4.07	4.29	1.42	**58.60**	15.63	24.39	163.37	1.39	**184.46**	**192.98**
APT (58)	**Range**	**12.85–36.60**	**71.72–347.62**	**82.78–897.43**	**11.40–55.13**	**42.60–129.46**	**29.21–1068.14**	**29.81–1519.56**	**12.15–163.19**	459.84–3003.92	**45.16–393.67**	**1.37–10.59**	**0.45–2.39**	**4.76–26.54**	**6.25–25.70**	**11.87–39.11**	**1.34–7.62**	73.30–474.78	**31.91–124.64**	**29.47–172.29**	**104.13–805.44**	**1.51–7.33**	168.83–1030.55	991.58–3542.98
	Avg.	**23.69**	**194.53**	**175.78**	**27.68**	**67.19**	**139.87**	**146.88**	**37.20**	**812.82**	**169.93**	**5.02**	**1.22**	**14.74**	**12.46**	**30.04**	**3.40**	**236.81**	**65.91**	**70.32**	**265.73**	**4.48**	**406.44**	**1456.73**
	STD (±)	**5.75**	**62.16**	**106.25**	**9.23**	**15.10**	**150.66**	**257.96**	**24.52**	**402.27**	**65.20**	**1.69**	**0.42**	**4.21**	**4.14**	**6.56**	**1.47**	**74.10**	**18.23**	**28.81**	**157.32**	**1.50**	**178.79**	**384.41**
East coast rivers draining DVT (4)	Range	23.89–26.25	156.52–201.09	117.10–142.33	26.27–33.86	72.84–77.17	71.48–228.60	324.38–467.08	17.38–47.34	**869.88–1101.33**	110.91–129.76	3.11–3.66	0.74–1.09	7.20–11.24	7.70–18.34	16.52–20.69	1.74–2.90	**156.24–177.61**	68.56–106.35	75.41–124.79	130.67–325.64	3.72–5.44	**301.89–549.25**	**1528.03–1818.88**
	Avg.	25.09	181.88	130.78	30.58	75.46	164.54	387.30	28.19	**1023.80**	119.43	3.30	0.88	9.33	12.76	19.26	2.17	**167.12**	91.86	103.64	235.32	4.71	**435.52**	**1626.44**
	STD (±)	1.17	18.60	11.33	3.15	1.89	70.05	59.92	13.15	**104.47**	7.78	0.25	0.16	1.67	4.35	1.94	0.52	**16.67**	16.35	21.64	87.04	0.72	**115.09**	**133.09**
West coast rivers draining DVT (21)	Range	26.37–58.58	194.68–465.37	86.19–267.99	27.04–70.84	53.67–104.42	133.71–275.27	64.06–192.93	8.60–39.25	**701.90–1290.95**	158.73–321.44	4.32–9.14	0.90–1.71	9.00–18.22	5.40–18.30	23.35–45.46	1–5.90	**225.35–402.31**	26.92–92.18	42.27–217.87	128.84–362.78	1.67–7.82	**230.14–464.08**	**1361.72–1981.02**
	Avg.	40.15	343.61	159.77	48.83	67.89	204.18	102.43	23.46	**990.31**	248.78	6.80	1.25	12.77	8.65	30.10	2.69	**311.04**	49.72	75.98	193.89	4.01	**323.61**	**1625.86**
	STD (±)	8.21	75.77	46.99	12.27	12.02	47.94	32.05	8.44	**133.75**	45.46	1.23	0.25	2.94	3.33	4.77	1.38	**49.59**	19.26	39.00	59.51	1.82	**62.83**	**164.40**
DVT (25)	**Range**	**23.89–58.58**	**156.52–465.37**	**86.19–267.99**	**26.27–70.84**	**53.67–104.42**	**71.48–275.27**	**64.06–467.08**	**8.60–47.34**	701.90–1290.95	**110.91–321.44**	**3.11–9.14**	**0.74–1.71**	**7.20–18.22**	**5.40–18.34**	**16.52–45.46**	**1–5.90**	156.24–402.31	**26.92–106.35**	**42.27–217.87**	**128.84–362.78**	**1.67–7.82**	230.14–549.25	1361.72–1981.02
	Avg.	**37.74**	**317.73**	**155.13**	**45.91**	**69.10**	**197.84**	**148.01**	**24.22**	**995.67**	**228.09**	**6.24**	**1.19**	**12.22**	**9.31**	**28.36**	**2.61**	**288.01**	**56.46**	**80.41**	**200.52**	**4.12**	**341.51**	**1625.96**
	STD (±)	**9.39**	**92.13**	**44.43**	**13.16**	**11.35**	**52.43**	**112.54**	**9.17**	**128.17**	**63.81**	**1.73**	**0.27**	**3.03**	**3.74**	**5.99**	**1.29**	**70.41**	**24.32**	**37.85**	**64.33**	**1.70**	**81.85**	**157.28**
East coast rivers draining MLT (4)	Range	14.89–20.99	94.87–141.72	101.38–142.52	19.58–40.87	58.12–70.21	57.27–104.42	113.83–199.89	32.91–40.76	**595.89–662.38**	65.94–103.96	1.79–2.83	0.75–1.14	7.96–12.54	12.77–19.76	15.79–21.89	1.97–3.56	**107.82–165.19**	99.79–139.21	47.38–78.51	257.20–549.52	8.10–9.58	**440.41–705.59**	**1168.26–1484.84**
	Avg.	18.88	123.11	124.79	25.90	63.05	76.29	159.28	36.17	**627.45**	90.02	2.46	1.03	10.86	16.13	19.94	2.76	**143.20**	121.77	64.28	353.09	8.82	**547.96**	**1318.61**
	STD (±)	2.77	20.43	18.91	10.07	5.85	19.99	40.45	3.45	**27.61**	16.60	0.46	0.19	2.04	3.46	2.81	0.67	**24.72**	18.84	13.03	134.97	0.61	**114.13**	**129.57**

Table 2. *Cont.*

Rivers		Sc	V	Cr	Co	Ni	Cu	Zn	Pb	∑TTE	Zr	Hf	Ta	Nb	Th	Ga	U	∑HFSE	Rb	Sr	Ba	Cs	∑LILE	∑TE
West coast rivers draining MLT (17)	Range	27.05–43.05	164.99–424.37	105.93–968.39	28.29–91.34	42.41–536.77	110.88–391.21	52.22–697.89	11.17–77.11	**590.30–3112.0**	182.27–270.61	4.95–7.04	0.97–1.58	11.19–15.16	6.82–14.28	23.01–30.96	1.14–2.44	**238.53–334.34**	41.54–101.18	83.44–374.89	163.61–382.99	3.45–8.56	**347.13–698.85**	**1249.82–3734.38**
	Avg.	36.24	264.24	172.99	40.26	75.47	165.34	117.30	21.67	**893.51**	221.23	5.90	1.22	13.05	8.73	25.96	1.58	**277.69**	65.38	129.26	225.60	5.02	**425.26**	**1597.76**
	STD (±)	3.93	73.68	205.49	13.68	118.93	66.20	151.43	15.57	**580.95**	22.51	0.58	0.16	1.09	1.77	1.94	0.33	**24.01**	15.48	65.98	56.85	1.20	**106.92**	**565.46**
MLT (21)	**Range**	**14.89–43.05**	**94.87–424.37**	**101.38–968.39**	**19.58–91.34**	**42.41–536.77**	**57.27–391.21**	**52.22–697.89**	**11.17–77.11**	**590.30–3112.70**	**65.94–270.61**	**1.79–7.04**	**0.75–1.58**	**7.96–15.16**	**6.82–19.76**	**15.79–30.96**	**1.14–3.56**	**107.82–334.34**	**41.54–139.21**	**47.38–374.89**	**163.61–549.52**	**3.45–9.58**	**347.13–705.59**	**1168.26–3734.38**
	Avg.	**32.93**	**237.35**	**163.81**	**37.53**	**73.10**	**148.38**	**125.30**	**24.43**	**842.84**	**196.24**	**5.25**	**1.19**	**12.64**	**10.14**	**24.82**	**1.81**	**252.07**	**76.12**	**116.88**	**249.88**	**5.74**	**448.63**	**1544.58**
	STD (±)	**7.89**	**87.35**	**184.96**	**14.08**	**106.52**	**69.64**	**137.39**	**15.16**	**530.64**	**56.87**	**1.49**	**0.18**	**1.54**	**3.63**	**3.17**	**0.62**	**59.00**	**27.56**	**64.74**	**89.16**	**1.88**	**116.35**	**520.51**
PIRAC (104)	Over all range	12.85–58.58	71.72–465.37	82.78–968.39	11.40–91.34	42.41–536.77	29.21–1068.14	29.81–1519.56	8.60–163.19	**459.84–3112.70**	45.16–393.67	1.37–10.59	0.45–2.39	4.76–26.54	5.40–25.0	11.87–45.46	1.14–7.62	**73.30–474.78**	26.92–139.21	29.47–374.89	128.84–805.44	1.51–9.58	**168.83–1030.55**	**991.58–3542.98**
	Over all avg.	**28.94**	**232.79**	**168.40**	**34.05**	**68.84**	**155.52**	**142.79**	**31.50**	**862.84**	**189.22**	**5.36**	**1.21**	**13.71**	**11.24**	**28.58**	**2.89**	**252.20**	**65.70**	**82.15**	**246.86**	**4.65**	**399.35**	**1515.15**
	Over all STD (±)	1.83	16.11	70.43	2.58	53.90	52.45	77.78	7.74	353.69	4.46	0.13	0.12	1.34	0.27	1.81	0.45	67.83	4.74	18.69	48.14	0.19	126.66	183.51
Reference Sedi-ments	**UCC**	**14.00**	**97.00**	**92.30**	**17.30**	**47.30**	**27.70**	**67.00**	**17.00**	**379.60**	**193.00**	**5.26**	**0.88**	**11.80**	**10.10**	**17.50**	**2.63**	**241.17**	**82.00**	**320.00**	**624.00**	**4.10**	**1030.10**	**1650.87**
	PAAS	**15.89**	**150.00**	**110.00**	**23.00**	**55.00**	**50.00**	**85.00**	**20.00**	**508.89**	**210.00**	**5.00**	**1.50**	**19.00**	**14.60**	**20.00**	**3.10**	**273.20**	**160.00**	**200.00**	**650.00**	**15.00**	**1025.00**	**1807.09**

APT: Archean–Proterozoic Terrain (this study); DVT: Deccan Trap Volcanic Terrain (this study); MLT: Mixed-Lithology Terrain (this study); PIRAC: Peninsular India Rivers Average Clay (this study); UCC: Upper Continental Crust [16]; PAAS: Post-Archean average Australian Shale [18].

4.3. Distribution of Rare Earth Elements (REE)

Table 3 shows REE data in the clay fraction of sediments in the rivers draining APT, DVT and MLT. ∑REE showed a broad range of values in the rivers of the west coast compared to that of the east coast. The average total rare earth element (∑REE) content of the clays increased from APT (184 µg/g) to DVT (195.5 µg/g) and then to MLT (231 µg/g) in the east coast rivers, but decreased from APT (180 µg/g) to DVT (162 µg/g) and then to MLT (142.6 µg/g) in the west coast rivers. The average ∑REE content of clay from all rivers (PIRAC: 173.2 µg/g) was higher than in UCC (148.96 µg/g) but lower than in PAAS (208.6 µg/g). Moreover, ∑REE showed strong correlation with LREE/HREE in river sediments of each terrain [29,30]. Figure 6 shows the PAAS-normalised average REE distribution in the clays from each terrain, in the clays from the east and west coast rivers, and in the clays from all rivers (PIRAC). The average REE patterns for APT were different for the east and west coast rivers (Figure 6). The LREE-depleted and MREE- and HREE-enriched pattern, with positive Ce and Eu anomalies, was characteristic of the east coast rivers. The west coast rivers showed LREE-enriched and MREE- and HREE-depleted pattern, with positive Ce and Eu anomalies. The average REE patterns for DVT were similar for the clays from the east and west coast rivers and display LREE-depleted and MREE- and HREE-enriched patterns with positive Ce and Eu anomalies. The average REE pattern for the clays from MLT showed MREE- and HREE-enriched, and slightly depleted LREE pattern, with positive Ce and Eu anomalies for the east coast rivers, and LREE-depleted and MREE- and HREE-enriched pattern, with positive Ce and Eu anomalies for the west coast rivers. The PAAS-normalised average REE of clays from all east coast and west coast rivers, and from all rivers (PIRAC), showed MREE- and HREE-enriched and LREE-depleted patterns with positive Ce and Eu anomalies.

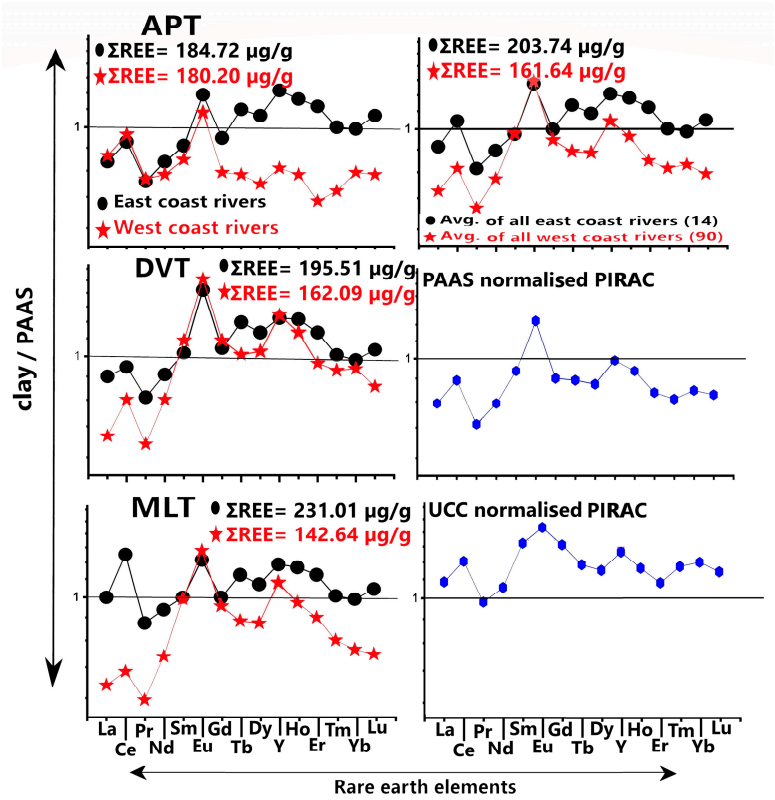


Figure 6. PAAS-normalised average rare earth element (REE) distribution in the clays from each terrain, in the clays from the rivers of the east and coast of India, and in the clays of all rivers (PIRAC). UCC normalised PIRAC is also shown.

Table 3. Rare earth element content (μg/g) of the clay fraction (<4 μm) of sediments in the rivers of the east coast and west coast of India.

Rivers		La	Ce	Pr	Nd	Sm	Eu	Gd	Tb	Dy	Y	Ho	Er	Tm	Yb	Lu	∑REE
East coast rivers draining APT (6)	Range	29.71–45.41	65.09–105.38	6.13–9.42	25.02–39.53	4.76–8.58	1.17–2.04	3.84–8.95	0.59–1.65	3.19–9.90	18.48–60.49	0.67–2.21	1.82–6.28	0.23–0.82	1.56–5.42	0.24–0.84	144.02–246.43
	Avg.	36.71	81.31	7.45	30.62	6.20	1.46	5.71	0.99	5.70	33.76	1.24	3.47	0.45	2.98	0.46	184.72
	STD (±)	5.61	15.37	1.20	5.14	1.34	0.31	1.95	0.43	2.78	17.37	0.63	1.84	0.24	1.58	0.24	36.04
West coast rivers draining APT (52)	Range	8.04–95.77	29.50–179.62	1.36–21.94	5.80–78.96	1.34–13.80	0.30–3.34	1.10–10.46	0.17–1.43	1.29–7.04	8.57–32.17	0.32–1.30	0.75–3.50	0.16–0.47	1.24–3.34	0.14–0.55	51.80–421.07
	Avg.	37.98	84.62	7.48	28.22	5.69	1.32	4.63	0.68	3.85	21.51	0.80	1.99	0.31	2.31	0.33	180.20
	STD (±)	20.32	32.32	4.52	15.02	2.47	0.60	2.03	0.31	1.47	6.12	0.25	0.84	0.09	0.56	0.11	78.69
APT (58)	**Range**	**8.04–95.77**	**29.50–179.62**	**1.36–21.94**	**5.80–78.96**	**1.34–13.80**	**0.30–3.34**	**1.10–10.46**	**0.17–1.65**	**1.29–9.90**	**8.57–60.49**	**0.32–2.21**	**0.75–6.28**	**0.16–0.82**	**1.24–5.42**	**0.14–0.84**	**51.80–421.07**
	Avg.	**37.85**	**84.28**	**7.47**	**28.47**	**5.74**	**1.34**	**4.74**	**0.71**	**4.04**	**22.78**	**0.85**	**2.14**	**0.33**	**2.38**	**0.34**	**180.67**
	STD (±)	**19.29**	**30.92**	**4.29**	**14.31**	**2.38**	**0.57**	**2.03**	**0.34**	**1.72**	**8.61**	**0.33**	**1.06**	**0.12**	**0.73**	**0.13**	**75.21**
East coast rivers draining DVT (4)	Range	23.34–63.18	54.83–126.78	5.31–11.93	23.26–48.01	5.19–9.44	1.45–2.26	4.96–8.38	0.86–1.39	4.83–7.73	27.39–44.29	1.03–1.64	2.82–4.42	0.36–0.56	2.38–3.58	0.36–0.55	130.98–289.85
	Avg.	39.46	83.34	8.05	33.65	7.02	1.78	6.35	1.08	6.09	34.17	1.30	3.54	0.45	2.95	0.45	195.51
	STD (±)	16.97	30.91	2.82	10.55	1.84	0.36	1.50	0.23	1.26	7.64	0.26	0.68	0.08	0.52	0.08	67.95
West coast rivers draining DVT (21)	Range	20.09–46.22	45.04–127.80	4.32–9.00	19.19–41.57	4.84–10.43	1.10–2.78	3.67–9.88	0.51–1.36	3.25–8.28	20.65–54.55	0.71–1.85	1.46–4.93	0.26–0.62	2.05–3.92	0.24–0.54	114.18–244.20
	Avg.	28.20	68.63	6.04	29.00	7.60	1.91	6.62	0.90	5.47	34.76	1.21	2.95	0.41	2.80	0.36	162.09
	STD (±)	6.90	19.88	1.23	5.75	1.56	0.46	1.66	0.22	1.31	8.95	0.29	1.00	0.09	0.47	0.07	32.55
DVT (25)	**Range**	**20.09–63.18**	**45.04–127.80**	**4.32–11.93**	**19.19–48.01**	**4.84–10.43**	**1.10–2.78**	**3.67–9.88**	**0.51–1.39**	**3.25–8.28**	**20.65–54.55**	**0.71–1.85**	**1.46–4.93**	**0.26–0.62**	**2.05–3.92**	**0.24–0.55**	**114.18–289.85**
	Avg.	**30.00**	**70.99**	**6.36**	**29.74**	**7.51**	**1.89**	**6.58**	**0.93**	**5.57**	**34.67**	**1.22**	**3.04**	**0.42**	**2.83**	**0.37**	**167.43**
	STD (±)	**9.66**	**21.89**	**1.68**	**6.67**	**1.58**	**0.44**	**1.61**	**0.23**	**1.30**	**8.61**	**0.28**	**0.97**	**0.09**	**0.47**	**0.08**	**40.20**
East coast rivers draining MLT (4)	Range	34.96–57.54	73.69–160.24	7.08–11.26	25.99–45.28	4.82–8.95	1.10–1.93	4.37–7.81	0.73–1.33	4.46–7.41	26.74–42.96	1.01–1.61	2.75–4.47	0.35–0.57	2.28–3.70	0.34–0.55	169.03–270.65
	Avg.	44.61	113.26	8.71	34.66	6.85	1.50	6.05	1.01	5.74	33.09	1.25	3.49	0.45	2.99	0.45	231.01
	STD (±)	10.52	36.29	2.12	8.93	1.87	0.38	1.56	0.27	1.40	7.59	0.29	0.78	0.09	0.59	0.09	44.42
West coast rivers draining MLT (17)	Range	20.98–35.59	47.12–71.31	4.63–6.77	22.27–29.97	6.04–7.47	1.33–1.79	5.10–6.31	0.68–0.84	4.07–5.01	26.26–32.46	0.90–1.11	2.45–2.97	0.32–0.38	2.01–2.39	0.28–0.33	118.54–167.96
	Avg.	26.78	57.51	5.62	26.51	6.85	1.59	5.76	0.77	4.60	29.64	1.01	2.74	0.35	2.23	0.31	142.64
	STD (±)	3.70	5.57	0.56	2.23	0.45	0.14	0.42	0.06	0.33	2.19	0.07	0.19	0.02	0.14	0.02	12.50
MLT (21)	**Range**	**20.98–57.54**	**47.12–160.24**	**4.63–11.26**	**22.27–45.28**	**4.82–8.95**	**1.10–1.93**	**4.37–7.81**	**0.68–1.33**	**4.07–7.41**	**26.26–42.96**	**0.90–1.61**	**2.45–4.47**	**0.32–0.57**	**2.01–3.70**	**0.28–0.55**	**118.54–270.65**
	Avg.	**30.17**	**68.13**	**6.21**	**28.06**	**6.85**	**1.57**	**5.82**	**0.82**	**4.81**	**30.30**	**1.06**	**2.88**	**0.37**	**2.38**	**0.34**	**159.47**
	STD (±)	**8.89**	**26.94**	**1.57**	**5.17**	**0.83**	**0.20**	**0.72**	**0.15**	**0.77**	**3.80**	**0.16**	**0.46**	**0.06**	**0.40**	**0.07**	**41.05**

Table 3. *Cont.*

Rivers		La	Ce	Pr	Nd	Sm	Eu	Gd	Tb	Dy	Y	Ho	Er	Tm	Yb	Lu	∑REE
PIRAC (104)	Over all range	8.04–95.77	29.50–179.62	1.36–21.94	5.80–78.96	1.34–13.80	0.30–3.34	1.10–10.46	0.17–1.65	1.29–9.90	8.57–60.49	0.32–2.21	0.75–6.28	0.16–0.82	1.24–5.42	0.14–0.84	51.80–421.07
	Over all avg.	**34.41**	**77.82**	**6.95**	**28.69**	**6.39**	**1.52**	**5.40**	**0.78**	**4.56**	**27.15**	**0.98**	**2.51**	**0.36**	**2.49**	**0.35**	**173.21**
	Over all STD (±)	5.80	4.53	1.54	4.90	0.77	0.19	0.67	0.09	0.47	2.78	0.09	0.33	0.03	0.18	0.04	19.97
Reference Sediments	**UCC**	**31.40**	**63.40**	**7.10**	**27.00**	**4.70**	**1.02**	**4.01**	**0.65**	**3.91**	**21.00**	**0.83**	**2.30**	**0.30**	**2.04**	**0.30**	**148.96**
	PAAS	**44.56**	**88.25**	**10.15**	**37.32**	**6.88**	**1.21**	**6.04**	**0.89**	**5.32**	**27.31**	**1.05**	**3.07**	**0.45**	**3.01**	**0.43**	**208.63**

LREE-La to Nd; MREE-Sm to Ho; HREE-Er to Lu [19]; APT: Archean–Proterozoic Terrain (this study); DVT: Deccan Trap Volcanic Terrain (this study); MLT: Mixed-Lithology Terrain (this study); PIRAC: Peninsular India Rivers Average Clay (this study); UCC: Upper Continental Crust [16]; PAAS: Post-Archean average Australian Shale [18].

5. Discussion

The chemical composition of river sediments largely depends on the nature of source rocks, intensity of chemical weathering and sorting during transport and deposition. Pollution and diagenesis also affect the geochemistry of sediments. The humid, tropical climate dominantly prevails over Peninsular India. Heavy monsoonal rainfall under tropical climate favours percolation of rainwater through source rocks, causing increase in the intensity of chemical weathering, leading to the alteration of minerals in source rocks. Intense chemical weathering causes quick solution of mobile elements (Ca, Mg, Na and K) and enrichment of immobile elements (Al, Fe and Ti) in the sediments.

5.1. Major Elements and Intensity of Weathering

Positive correlation of CIA with Al_2O_3 and TiO_2 and negative correlation of CIA with Fe_2O_3, MgO, K_2O and CaO (Figure 4) suggests that the intensity of weathering played a major role in the depletion of mobile elements and enrichment of immobile elements in the clays. Low and variable SiO_2/Al_2O_3 of our samples compared to that in UCC and PAAS (Table 1) also suggest varied intensity of chemical weathering from south to north Peninsular India. Much low average SiO_2/Al_2O_3 for the clays from APT (1.95) and DVT (2.54) of the west coast rivers resembles laterite soils (1.33 to 2.22; [66]), suggesting advanced chemical weathering or lateritic weathering. The average SiO_2/Al_2O_3 for the clays from APT (2.72) and MLT (2.69) of the east coast rivers also suggests intense or strong chemical weathering. Relatively high SiO_2/Al_2O_3 for DVT clays (3.06) from the east coast rivers and MLT clays (3.29) from the west coast rivers (but lower than in UCC and PAAS) suggests non-lateritic, chemical weathering with moderate intensity. The low average SiO_2/Al_2O_3 of PIRAC (2.29) compared to UCC and PAAS suggests that the continental crust of Peninsular India, in general, experienced advanced to intense chemical weathering. The intensity of chemical weathering is well illustrated in (A-CN-K) and ((A-K)-C-N) ternary diagrams (Figure 3A,B). For example, plotting of CIA and PIA values close to apex A for the clays from the west coast rivers draining APT and DVT suggests strong chemical weathering and high degree of plagioclase weathering. A gradual shift in the intensity of weathering is also displayed in these diagrams, where CIA and PIA values plot away, and much away from apex A both in the west- and east-flowing rivers, indicating lateritic to strong weathering in APT, strong to intermediate weathering in DVT and intermediate weathering in MLT. The A-CNK-FM diagrams (Figure 3C) also display the trend in the intensity of weathering. For example, plotting of all samples away from apex CNK indicates that the mobile elements (Ca, Na and K) are leached away suggesting advanced chemical weathering. The clays from APT and DVT plot parallel to A-FM line and more towards apex A in this diagram (Figure 3C), implying enrichment of Al and to some extent Fe and/or Mg. This indicates relative enrichment of aluminous (gibbsite, kaolinite) and ferruginous (hematite and goethite) minerals in highly weathered soils like laterites. The presence of goethite and gibbsite in the APT clays from the west coast rivers also argues in favour of lateritic weathering [46]. The clays from MLT plot slightly away from A-FM line and more towards PAAS value, indicating loss of Fe and/or Mg in the soils. Relatively high SiO_2, TiO_2, Fe_2O_3, MgO, MnO and Na_2O, and low CaO and P_2O_5 in the clays from east coast rivers compared to those of west coast rivers, upon PAAS normalisation, suggest prolonged chemical weathering on a gentle slope, and long transportation history lead to the solution of plagioclase feldspar and formation of mature sediments rich in quartz and oxides of Fe, Mn and Ti.

5.2. Controls of Source Rocks and Weathering in Trace Element Distribution

Trace element chemistry is controlled largely by source rocks and intensity of weathering [67]. Trace elements with high solubilities are fractionated rapidly during sedimentary processing, and elements with low solubilities are incorporated in secondary minerals such as clays or oxyhydroxides [19,68,69]. Trace elements usually associate with fine-grained clays and heavy minerals in the sediments. High average ∑TE (higher than in PAAS and UCC) corresponding to the clays from APT and DVT terrains of the east coast suggests trace elements contribution from different sources. High ∑TE is largely due to very high Cu, Zn and Pb in all terrains (Figure 5). They are pollution-associated elements and usually adsorb onto clay minerals and oxyhydroxides of Fe and Mn. The mean enrichment factor of the trace metals with reference to PAAS showed Cu and Zn are in the range of significant pollution and Pb in moderate pollution in APT and Cu and Zn in the range of moderate pollution in DVT [40]. These metals are in the range of minimum pollution in MLT clays. The ores of Fe–Mn and Cr oxides and Cu, Zn and Pb sulphides have been reported in the Singhbhum craton [70–72], corresponding to the Mixed-Lithology Terrain (MLT). In view of the above, Babu et al. [40] interpreted that the high Cu, Zn and Pb in the clays are due to anthropogenic pollution in southeast Indian rivers and erosion of sulfidic minerals and ore deposits from the hinterland in the northeast Indian rivers.

The Zr, Hf, Ta and Nb are depleted relative to PAAS in the clays from east coast rivers (Figure 5). These are high-field strength elements (HFSE), usually associated with heavy minerals, which largely confine to the coarser fractions of the sediment. The sediments of the east coast rivers experienced long transportation and recycling history. Therefore, their depletion in the clays of east coast rivers may be because heavy minerals containing these trace metals have settled much before in the river course, rather than being transported to and deposited at the lower reaches of the rivers. The slightly lower or similar values of Th, Ga and U as that of PAAS may be due to the adsorption of Th and Ga onto clays and U content influenced by ore material [73,74]. On the other hand, the average ∑TE increased from APT to MLT in the west coast rivers (Table 2). Here, increasing ∑TE corresponds to decreasing CIA. In general, the Archean–Proterozoic rocks contain relatively low trace element and high REE content compared to the Deccan Trap Volcanic rocks. Therefore, increasing ∑TE from APT to DVT may be related to source rocks. The Fe and Ti minerals such as magnetite, rutile and ilmenite (abundant in Deccan Traps) may have contributed high trace element content in DVT. Heavy rainfall on the steep slopes of the Western Ghats may have favoured release of trace elements from the parent rocks and been carried away quickly before being incorporated in clay minerals. Relatively high ∑TE, low CIA and high ICV values for MLT clays of the west coast suggest moderate weathering and immature sediments. Indeed, the rocks from MLT are volumetrically Deccan Traps, despite Proterozoic rocks and alluvial sediments being exposed in the drainage basins of the rivers (Figure 1). Arid climate prevails over this region. High ∑TE content and high ICV in MLT could be due to the dominance of mafic Deccan Trap material (with high Fe and Mg), which weather far more easily and quickly than the granitic and gneissic rocks and sediments weathered from arid conditions. The much depleted large-ion lithophile elements (Rb, Sr, Ba and Cs) in the clays from all terrains suggest their leaching because of the intense chemical weathering. PAAS-normalised trace element distribution of PIRAC showed high TTE and low HFSE and LILE, indicating dominance of mafic component material in the sediments.

5.3. Controls of Rare Earth Elements

Our studies on REEs of river sediments indicate that ∑REE is not dependent on the size of the drainage basin or the amount of detrital material supplied by rivers, but depends

on mineral composition of the clays [30,40]. The sources for REEs include heavy minerals, (monazite, apatite), ore deposits, mica and K-feldspar, REE associated with clay mineral lattice, and REEs adsorbed onto clays, Fe-Mn oxy hydroxides, phosphate and lateritic debris [30,40,47].

Contrasting distribution of ∑REE and ∑TE (high ∑REE coinciding with low ∑TE) also suggests ∑REE is related to the mineral composition of the sediments. Near similar average ∑REE for APT in the rivers of the east (184 µg/g) and west coasts (180 µg/g) (Table 3) suggest mineral composition of the terrain is an important factor determining REE content. As we move from south to north along the east coast of India, the rivers draining DVT consist of dominant Deccan Traps followed by felsic granites and high-grade metamorphic rocks, khondalites (garnet-sillimanite gneiss) of the Eastern Ghat mobile belt (rich in Fe-Mn ores). The river-draining MLT consists of Archean ore deposits of Fe-Mn and Cr oxides and Cu, Zn and Pb sulfides, followed by Precambrian felsic granites and charnockites. The increasing ΣREE in DVT and MLT could be due to increasing REE contribution from felsic granites and Fe-Mn oxide ores and sulfide ores [40]. It is well known that the felsic granites contain REE-rich heavy minerals and therefore high REE in the sediments. On the west coast, high ΣREE correlates with Th and P_2O_5 in the clays from APT, indicating heavy minerals (monazite and apatite) contributed REE [30,47]. Strong positive correlation of ΣREE with LREE/HREE in APT clays suggests that LREE-rich heavy minerals controlled REE content [29,30]. On the other hand, strong correlation of ΣREEs with Al_2O_3 and Fe_2O_3 and moderate correlation with MnO, K_2O, P_2O_5 and TiO_2 in the clays from DVT indicates that most of the REEs reside in the clay mineral lattice while a small part is adsorbed onto the surfaces of secondary weathering products such as Mn–Fe oxyhydroxides and phosphate minerals [47].

PAAS-normalised REE patterns: The MREE-enrichment in the clays from all terrains (Figure 6), has been attributed to the influence of (a) intense chemical weathering on source rocks in a tropical climate [75], (b) weathering of phosphate minerals in the drainage basin [41,76], and (c) analysis of clay fraction, which usually show high MREE and HREE enrichment compared to the bulk sediment [36].

The REE patterns of the clays from Archean–Proterozoic Terrain (APT) showed LREE enrichment over HREE in the west coast rivers and HREE enrichment over LREE in the east coast rivers (Figure 6). Advanced to intense chemical weathering is characteristic of the clays from APT. Moreover, REEs fractionate during chemical weathering. Since LREE are less mobile than HREE, more LREE are retained with the weathering residue, and HREE is carried away as complexions. The laterite profiles indeed exhibit strong REE fractionation with LREE-enrichment over HREE [77]. The hinterland rocks are dominantly felsic in the southern Peninsular India, which contribute to the LREE-enriched and HREE-depleted REE patterns. Therefore, LREE-enriched pattern in the west coast rivers draining APT is in agreement with the source rocks and lateritic weathering.

The HREE enrichment over LREE from APT clays of the east coast rivers is an average pattern of the clays from six rivers. The near equal proportions of LREE and HREE in the clays of Cauvery and Pennar rivers may be due to admixture of clays from different sources upon long transportation. It is likely that the weathering products from mafic rocks (basic and ultrabasic intrusions and garnetiferous gneisses) are admixed with those from the primary felsic rocks, resulting in flat REE pattern. The Ponnaiyar and Palar rivers are small and drain mono (felsic) lithology rocks and therefore show LREE-enriched and HREE-depleted pattern. The Nagavali and Vamsadhara Rivers drain khondalites (garnet-sillimanite gneiss) of the Eastern Ghats mobile belt that contain Fe-Mn ores. HREE enrichment is characteristic of both Fe-Mn ores and garnets [78,79]. The LREE-depleted and HREE-enriched pattern is an average pattern of six rivers, implying an overall enrichment

of mafic component in these clays. The positive Eu anomaly is characteristic of clays from APT, both in the rivers of the east and west coasts. (Figure 6). Felsic granitic rocks typically display a negative Eu anomaly because plagioclase fractionation or retention leaves the melt depleted in Eu. A positive Eu anomaly can appear in felsic-derived sediments if the source granite is a cumulate (enriched in accumulated plagioclase crystals), or if deep-crustal felsic granulites/tonalite-trondhjemite-granodiorite (TTG) residues rich in feldspar supply the detritus [20]. Felsic granulites from Archean terrains have substantial positive Eu anomaly. Since TTG-type Peninsular gneisses, dioritic to tonalite gneiss and granulite grade charnockites occur in the hinterland rocks [42], plagioclase may have accumulated in the APT clays, leading to positive Eu anomaly.

The average clays from DVT exhibit HREE-enriched and LREE-depleted REE pattern with positive Ce and Eu anomalies, both in the east and west coast rivers (Figure 6). The LREE-depleted and HREE-enriched pattern with positive Eu anomaly has been reported in the sediments derived from basic/mafic igneous rocks (basalts and gabbros) [20,22,36,80]. However, positive Ce anomaly is not a characteristic of volcanic rocks. In other words, DVT clays contain high proportions of mafic component-dominated material derived from Deccan Traps with some material from felsic granites.

The average clay from MLT exhibits slightly enriched HREE over LREE in the east coast rivers, and MREE- and HREE-enriched and LREE-depleted pattern in the west coast rivers. The clays from Archean ore deposits (Fe, Mn and Cr oxides) are admixed with Precambrian granitic metamorphic rocks in the east coast resulting in a mixed REE pattern with slight enrichment of HREE over LREE. On the other hand, Deccan Trap-dominated material is dominant in the clays from MLT of the west coast rivers, resulting in HREE-enriched and LREE-depleted REE pattern.

The PAAS-normalised REE of PIRAC is characterised by MREE- and HREE-enriched and LREE-depleted pattern, with Ce and Eu anomaly (Figure 6). Since PIRAC composition is an average composition of clays from 104 rivers draining Peninsular India, it is indeed an admixture of dominant mafic component material with some contribution from felsic source material. The dominance of mafic/felsic component in the sediments has also been verified from standard plots and element-to-element ratios. For example, the plot of Al_2O_3 and TiO_2 values in the clays of all rivers on the binary diagram of Bhatia [81] shows that most of the samples fall in the intermediate region between felsic and mafic provenance, with a few samples falling in the felsic provenance (Figure 7A). Similarly, the plot of TiO_2, MgO and Fe_2O_3 values of our samples in the TiO_2 versus Fe_2O_3 + MgO diagram of Bhatia [81] indicates that the samples from all terrains plot more towards basalts, suggesting dominance of the mafic component (Figure 7B). Felsic rocks are enriched with Th, whereas the basic igneous rocks are enriched with Sc. The plot of Th and Sc from the clays of all rivers on the Th vs. Sc diagram of Cullers [82] (Figure 7C) indicates a few samples plot in the felsic region and all other samples extend from intermediate region between felsic and mafic to mafic region. Similarly, the samples extend from granodiorite to basaltic region in the Th/Sc vs. Sc diagram (Figure 7D). Babu et al. [29,46,48] showed several ratio–ratio plots of trace elements to understand the dominance of mafic or felsic component in the sediments and reported dominance of mafic component in the large number of river samples, both from the east and west coasts of India.

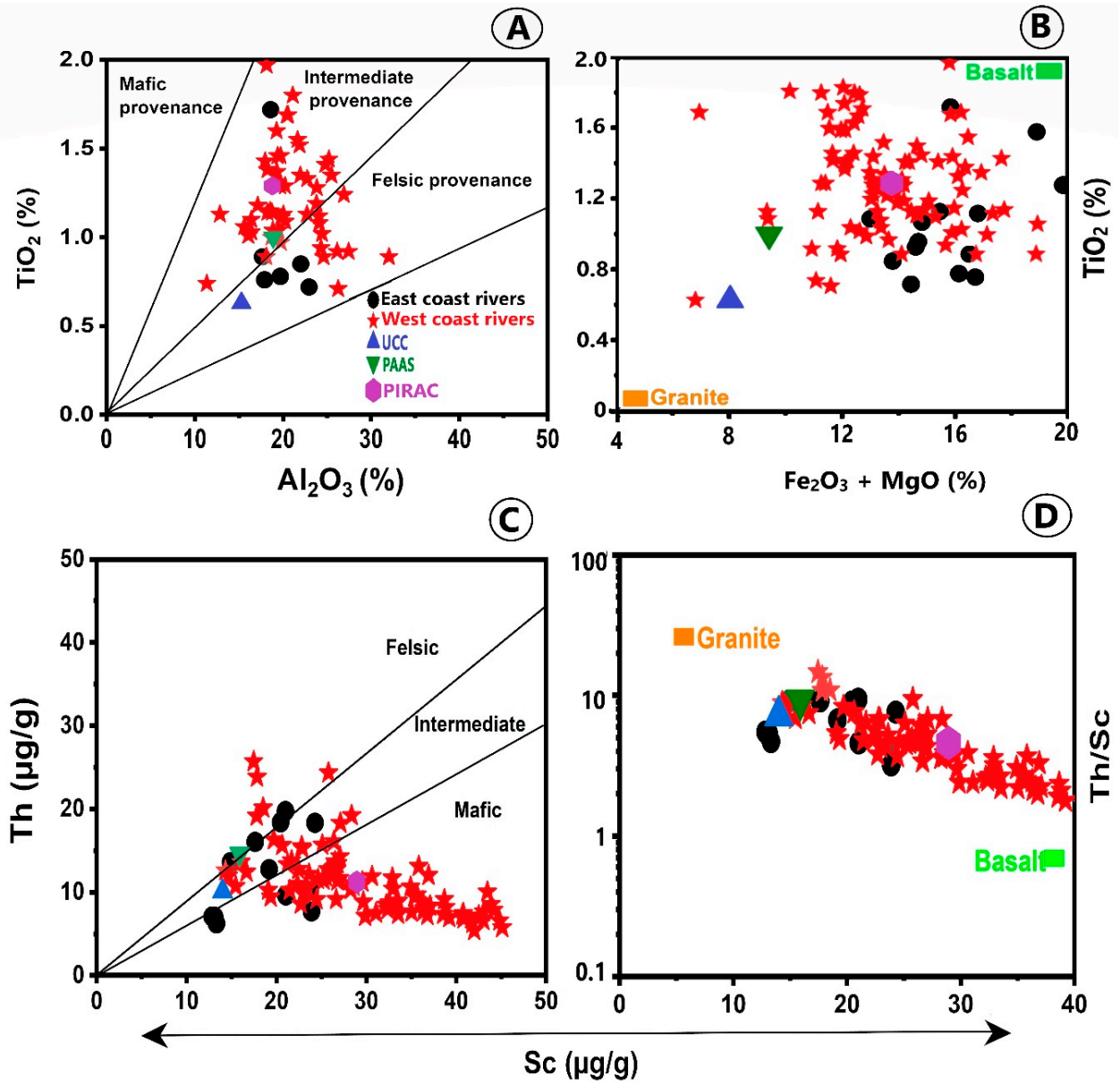


Figure 7. Geochemical provenance discrimination diagrams for the clay fractions of sediments in all the rivers. (**A**) Al_2O_3 versus TiO_2, with felsic, intermediate, and mafic provenance field [12,20]; (**B**) (Fe_2O_3 + MgO) versus TiO_2 [20]; (**C**) Sc versus Th [80]; and (**D**) Sc versus Th/Sc [39,83].

Ternary diagrams using trace metals are also helpful to distinguish the dominant trend of the source components in the sediments. In the La-Th-Sc diagram of Bhatia and Crook [84], the samples plot from granodiorite to more towards basalts (Figure 8A). Figure 8B shows the plot of V, Ni and Th × 10 data in the ternary diagram [85]. All samples plot in the region between felsic and mafic rocks and more towards mafic rocks. Figure 8C shows the plot of Zr, Cr and Ga values in the ternary diagram [86]. All samples plot parallel to the Cr-Zr axis and extend from sedimentary rocks to Basic rocks, with few samples extending towards Cr. Most of the samples are clustered in the region of basic rocks, implying dominance of mafic material. The dominance of mafic component in the sediments from Indian rivers has been reported previously [29,41,44,48,87], and it has been interpreted that the crystalline felsic components weathered from granitic terrain deposited more closely to the source, and finer mafic component, easily weathered from source rocks, is transported farther from the source and settled at the lower reaches of the rivers.

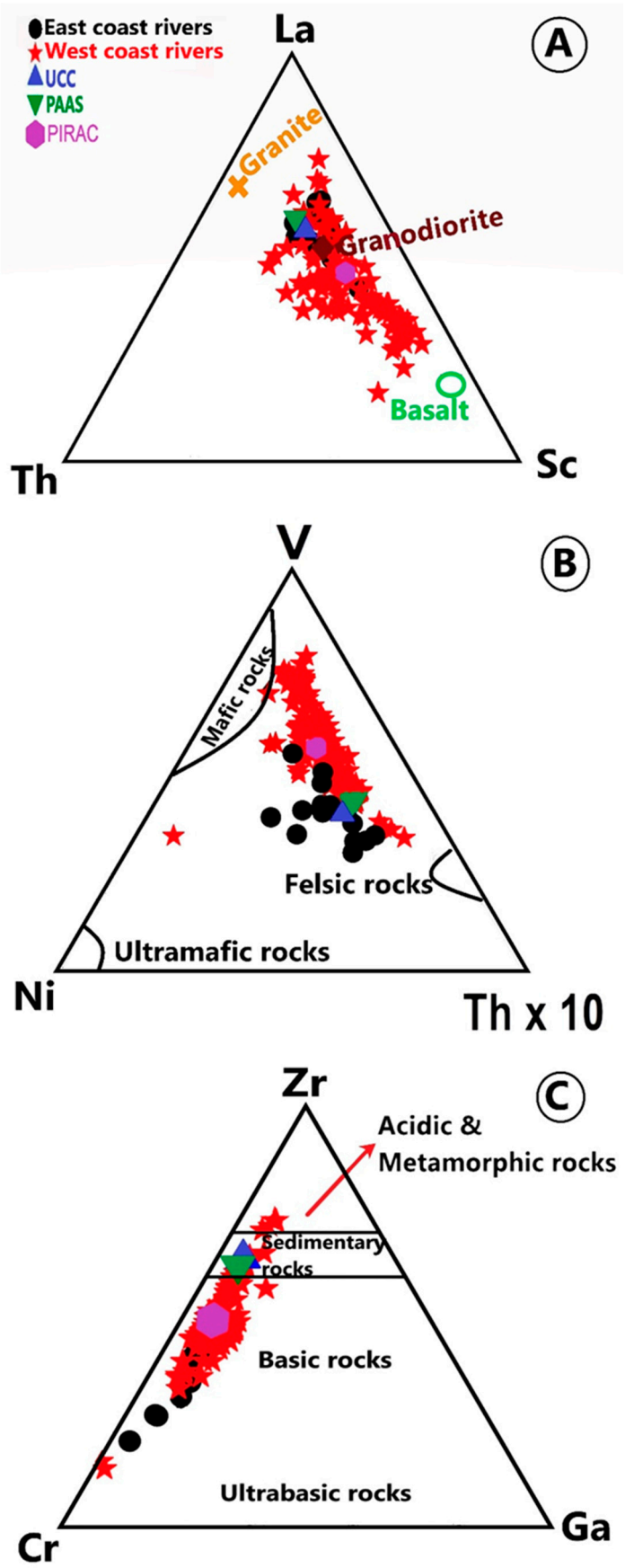


Figure 8. Ternary diagrams of trace elements used for provenance discrimination: (**A**) La–Th–Sc [81,85]; (**B**) V–Ni–Th × 10 [85] and (**C**) Zr–Cr–Ga [86].

5.4. The Geochemical Composition of PIRAC

The PAAS-normalised major, trace and rare earth element distribution of PIRAC shows low Si, Ca and K, high Fe, Mn, Mg, Na, Ti and P and near similar Al content (Figure 2), high transition trace elements (TTE), low high field strength elements (HFSE) and large-ion lithophile elements (LILE) (Figure 5), and MREE- and HREE-enriched and LREE-depleted pattern with positive Ce and Eu anomalies (Figure 6). PIRAC represents the downstream clays, which are strongly weathered and controlled by strong hydrodynamic sorting, resulting in mafic component dominated material. Therefore, the PAAS-normalised REE pattern of PIRAC is different from that of upper continental crust (UCC) [15,16] and East China Post-Archean Shale (ECPAS) [34], which show LREE-enriched and HREE-depleted REE pattern (Figure 9A). The World Rivers Average Clay (WRAC) [36] is also weathered and long-distance-transported clay from world rivers. Since the REE pattern of PIRAC is different from that of WRAC, the composition of PIRAC probably represents regional chemical characteristics of the average sediment from Peninsular India. The REE pattern of PIRAC resembles that of European shale (ES) [32] and Mud of Queensland (MUQ) [33] and North American Shale Composite (NASC) [31], except in the absence of significant Ce anomaly in ES and MUQ (Figure 9A). The sediments from the large rivers of the world result from efficient mixing of various provenance components from the upper crust [37,38,88]. The PAAS-normalised REE pattern of the sediments from the world's large tropical rivers shows LREE-enriched and MREE- and HREE-depleted pattern, similar to that of the UCC, but different from PIRAC (Figure 9B). Although the Archaean and Precambrian metamorphic crust is widely scattered and voluminously abundant in the drainage basins of several rivers, the MREE- and HREE-enriched and LREE-depleted REE pattern of PIRAC suggest dominance of mafic component material at the lower reaches of several rivers. It implies the lithology (vulnerability for easy erosion), intensity of weathering and size sorting during transportation controlled the geochemical characteristic of the clays deposited at the lower reaches of rivers.

Figure 9C shows the PIRAC-normalised REE patterns of the clays from major rivers of Peninsular India. It exhibits near equal proportions of LREE ($(La/Yb)_n$ = 1.04) and HREE ($(Lu/La)_n$ = 1.08) with negative Eu anomaly for the Cauvery River and LREE-enriched and HREE-depleted patterns for Godavari ($(La/Yb)_n$ = 1.28; $(Lu/La)_n$ = 0.86) and Mahanadi ($(La/Yb)_n$ = 1.12; $(Lu/La)_n$ = 0.95) Rivers, with negative Eu anomaly. Negative Eu anomaly is characteristic of felsic granites present in the drainage basins of these rivers. This indicates that the clays represent mixed sources, with slightly higher proportions of felsic source material. The $^{87}Sr/^{86}Sr$ of the clays from Cauvery (0.7146), Godavari (0.7255) and Mahanadi (0.7399) are within the values of upper continental crust (0.711–0.731; [89]) and average of the clays from world rivers (0.716; [90]), suggesting dominance of older crust material. However, the ϵ_{Nd} of the clay (−10.41), silt (−21.25) and sand (−23.05) fractions of the sediment from Godavari indicates mixed sources, an admixture of older and younger source sediment [91]. The PIRAC-normalised REE of the clays from the Krishna River, east coast of India, and Narmada and Tapti Rivers of the west coast of India indeed show LREE-depleted and MREE- and HREE-enriched pattern with positive Eu anomaly, indicating dominant sediment contribution from the Deccan Trap volcanic rocks. The clay mineralogy and Sr-Nd isotopes of the sediment from Krishna [92], Narmada and Tapti Rivers point to volcanic source [93]. We found that the PIRAC-normalised REEs are better illustrations of source sediments, relative to the other reference sediments. Therefore, the composition of PIRAC serves as a regional reference for river sediments of Peninsular India.

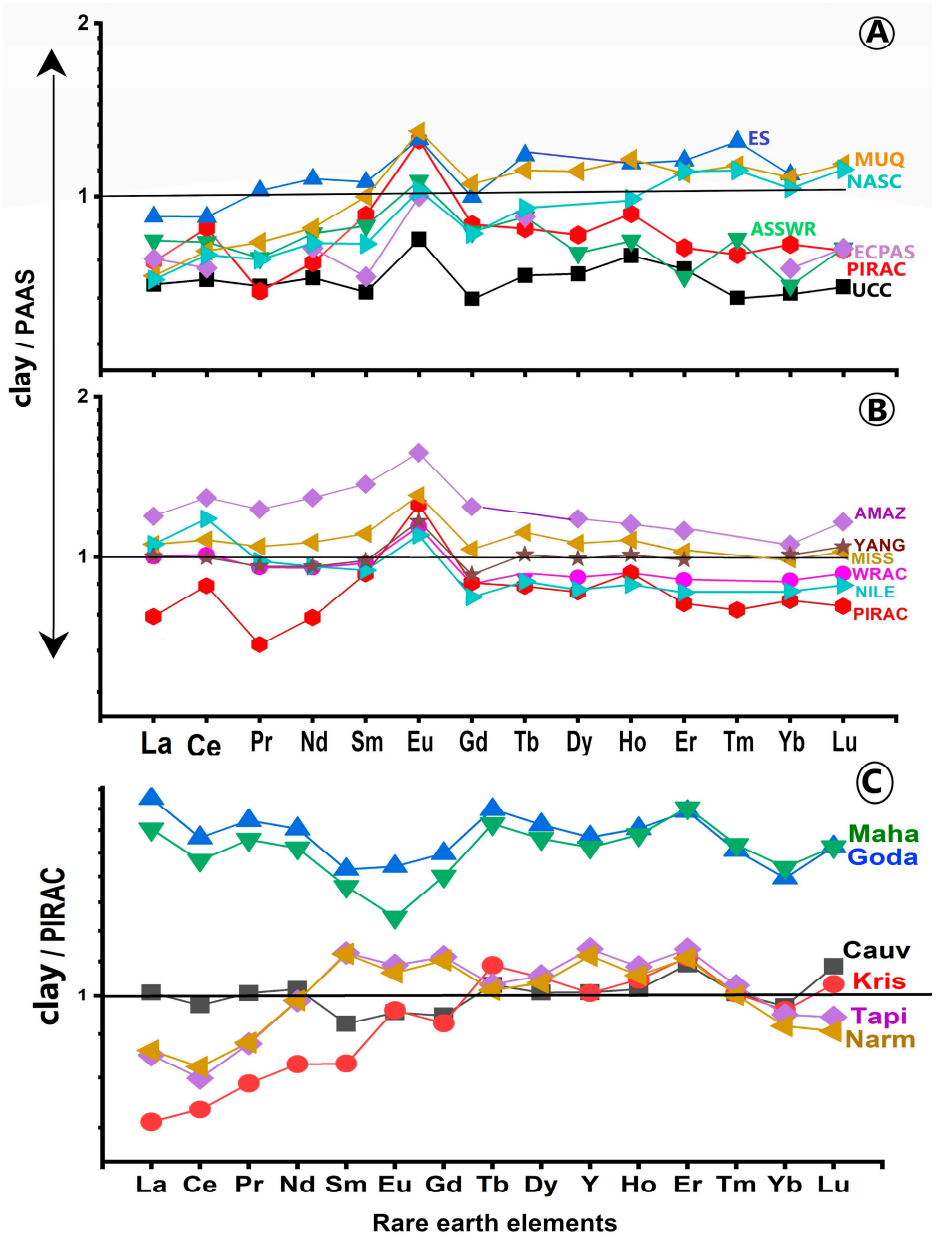


Figure 9. (**A**) PAAS-normalised REE of PIRAC together with Upper Continental Crust (UCC), European Shale (ES), Mud of Queensland (MUQ), North American Shale Composite (NASC), East China Post-Archean Shale (ECPAS) and Average Suspended Sediment of World Rivers (ASSWR). (**B**) PAAS-normalised REE patterns of PIRAC together with that of the clays from large tropical rivers of the world (Amazon, Nile, Mississippi, and Yangtze). REE data for the Amazon, Nile, Mississippi, and Yangtze rivers are from Bayon et al. [36]. (**C**) PIRAC-normalised REE patterns of the clays from major rivers of Peninsular India. Cauv: Cauvery River, Kris: Krishna River, Goda: Godavari River, Maha: Mahanadi River, Tapi: Tapati River, Narm: Narmada River.

6. Conclusions

The rivers of Peninsular India originate in the mountain/hill ranges or high plateaus, drain continental rocks and bring sediment load either to the Bay of Bengal or Arabian Sea. The geochemical compositions of the clay fraction of sediments from 104 rivers along the east and west coasts of India were examined to understand their regional variations and Peninsular India as a whole (PIRAC).

1. The clays from all rivers are depleted with mobile elements and enriched with immobile elements, relative to PAAS. The clays from the east coast rivers showed higher Si, Al, Fe, Mn, Mg, Na and K and lower Ti, Ca and P than those in the west coast.
2. Trace elements showed higher transition trace elements (∑TTE), lower high-field strength elements (∑HFSE) and large-ion lithophile elements (∑LILE), relative to PAAS. Elements such as Zr, Hf, Ta and Nb are much lower in the east coast rivers than those in the west coast.
3. The average ∑REE content is much higher in the east coast rivers than those in the west coast.
4. The PAAS-normalised REE of PIRAC showed LREE-depleted, MREE- and HREE-enriched pattern, with positive Ce and Eu anomalies.
5. The intensity of chemical weathering, erosion and transportation of easily eroded mafic rocks relative to that of felsic rocks resulted in deposition of mafic component-dominated material at the lower reaches of almost all rivers.
6. The composition of PIRAC is significantly different from other reference sediments.
7. The PIRAC-normalised REEs of the clays from major rivers are better illustrations of source sediments than other reference sediments.
8. The geochemical composition of PIRAC serves as a regional reference for river sediments of Peninsular India.

Author Contributions: Conceptualisation, V.P.R. and S.S.B.; methodology, S.S.B., V.P.R. and M.R.M.; software, S.S.B. and M.R.M.; validation, S.S.B., V.P.R. and M.R.M.; formal analysis, S.S.B., M.R.M. and V.P.R.; investigation, S.S.B., V.P.R. and M.R.M.; resources, V.P.R., S.S.B. and M.R.M.; data curation, S.S.B., V.P.R. and M.R.M.; writing—original draft preparation, V.P.R., S.S.B. and M.R.M.; writing—review and editing, V.P.R., S.S.B. and M.R.M.; visualisation, V.P.R., S.S.B. and M.R.M.; supervision, V.P.R., S.S.B. and M.R.M. All authors have read and agreed to the published version of the manuscript.

Funding: This work was carried out under the project "INSA-Senior Scientist funded by the Indian National Science Academy, New Delhi".

Data Availability Statement: The research data utilised in this study is given in the form of tables.

Acknowledgments: The authors thank the Vice-chancellor, VFSTR, Vignan's University and Director CSIR-NGRI for their encouragement. This work was carried out for the project awarded to VP Rao under the 'INSA-Senior Scientist' program by the Indian National Science Academy, New Delhi, and during the faculty position of Sk. Sai Babu at K.S.R.M. College of Engineering. We acknowledge the organisations for their financial support.

Conflicts of Interest: The authors declare no conflict of interest.

References

1. Alam, S.; Sama, A.K.; Prudhvi Raju, K.N. Is 'Peninsular India' a geographic expression? *Ann. Natl. Assoc. Geogr. India* **2022**, *42*, 198–206. [CrossRef]
2. Kumar, Y. Climatic conditions of India. *Int. J. Lead. Res. Publ.* **2025**, *6*, IJLRP25011238.
3. Dey, P.; Mujumdar, P.P. On the uniformity of rainfall distribution over India. *J. Hydrol.* **2019**, *578*, 124017. [CrossRef]
4. Pettijohn, F.J.; Potter, P.E.; Siever, R. *Sand and Sandstone*; Springer-Verlag: New York, NY, USA, 1972.
5. McLennan, S.M.; Hemming, S.; McDaniel, D.K.; Hanson, G.N. Geochemical approaches to sedimentation, provenance, and tectonics. In *Processes Controlling the Composition of Clastic Sediments*; Johnsson, M.J., Basu, A., Eds.; Geological Society of America Special Paper 284; GSA: Boulder, CO, USA, 1993; pp. 21–40.
6. Cox, R.; Lowe, D.R.; Cullers, R.L. The influence of sediment recycling and basement composition on evolution of mudrock chemistry in the southwestern United States. *Geochim. Cosmochim. Acta* **1995**, *59*, 2919–2940. [CrossRef]
7. Borges, J.B.; Huh, Y.; Moon, S.; Noh, H. Provenance and weathering control on river bed sediments of the eastern Tibetan Plateau and the Russian Far East. *Chem. Geol.* **2008**, *254*, 52–72. [CrossRef]

8. Garzanti, E.; Andó, S.; France-Lanord, C.; Censi, P.; Vignola, P.; Galy, V.; Lupker, M. Mineralogical and chemical variability of fluvial sediments 2. Suspended-load silt (Ganga–Brahmaputra, Bangladesh). *Earth Planet. Sci. Lett.* **2011**, *302*, 107–120. [CrossRef]
9. Liu, Z.; Colin, C.; Huang, W.; Le, K.P.; Tong, S.; Chen, Z.; Trentesaux, A. Climatic and tectonic controls on weathering in south China and Indochina Peninsula: Clay mineralogical and geochemical investigations from the Pearl, Red, and Mekong drainage basins. *Geochem. Geophys. Geosyst.* **2007**, *8*, Q05005. [CrossRef]
10. Liu, Z.; Wang, H.; Hantoro, S.W.; Sathiamurthy, E.; Colin, C.; Zhao, Y.; Li, J. Climatic and tectonic controls on chemical weathering in tropical Southeast Asia (Malay Peninsula, Borneo, and Sumatra). *Chem. Geol.* **2011**, *291*, 1–12. [CrossRef]
11. Babechuk, M.G.; Widdowson, M.; Kamber, B.S. Quantifying chemical weathering intensity and trace element release from two contrasting basalt profiles, Deccan Traps, India. *Chem. Geol.* **2014**, *363*, 56–75. [CrossRef]
12. Absar, N.; Sreenivas, B. Petrology and geochemistry of greywackes of the 1.6 Ga Middle Aravalli Supergroup, northwest India: Evidence for active margin processes. *Int. Geol. Rev.* **2015**, *57*, 134–158. [CrossRef]
13. Rashid, S.A.; Ahmad, S.; Singh, S.K.; Absar, N. Elemental and Sr–Nd isotopic geochemistry of Mesoproterozoic sedimentary successions from NE Lesser Himalaya, northern India: Implications for Proterozoic climate and tectonics. *J. Asian Earth Sci.* **2018**, *163*, 235–248. [CrossRef]
14. Babechuk, M.; Fedo, C. Analysis of chemical weathering trends across three compositional dimensions: Applications to modern and ancient mafic-rock weathering profiles. *Can. J. Earth Sci.* **2022**, *60*, 839–864. [CrossRef]
15. Taylor, S.R.; McLennan, S.M. Composition and evolution of the continental crust: Constraints from sedimentary rocks. In *Encyclopedia of Physical Science and Technology*, 3rd ed.; Meyers, R.A., Ed.; Academic Press: San Diego, CA, USA, 2001; pp. 697–719.
16. Rudnick, R.L.; Gao, S. Composition of the continental crust. In *Treatise on Geochemistry, Vol. 3: The Crust*; Rudnick, R.L., Ed.; Elsevier-Pergamon: Oxford, UK, 2003; pp. 1–64.
17. Nance, W.B.; Taylor, S.R. Rare earth element patterns and crustal evolution-I. Australian post-Archean sedimentary rocks. *Geochim. Cosmochim. Acta* **1976**, *40*, 1539–1551. [CrossRef]
18. Pourmand, A.; Dauphas, N.; Ireland, T.J. A novel extraction chromatography and MC-ICP-MS technique for rapid analysis of REE, Sc and Y: Revising CI-chondrite and Post-Archean Australian Shale (PAAS) abundances. *Chem. Geol.* **2012**, *291*, 38–54. [CrossRef]
19. Taylor, S.R.; McLennan, S.M. *The Continental Crust: Its Composition and Evolution*; Blackwell Scientific Publications: Palo Alto, CA, USA; Malden, MA, USA, 1985; p. 312.
20. McLennan, S.M. Rare earth elements in sedimentary rocks: Influence of provenance and sedimentary processes. In *Geochemistry and Mineralogy of Rare Earth Elements*; De Gruyter: Berlin, Germany, 1989; Volume 21, pp. 169–200. [CrossRef]
21. Martins, M.V.A.; Rocha, F. Rare earth elements as fingerprints of differentiated sediment sources in the Ria de Aveiro (Portugal). *J. Sediment. Environ.* **2016**, *1*, 17–42. [CrossRef]
22. Goldstein, S.J.; Jacobsen, S.B. Rare earth elements in river waters. *Earth Planet. Sci. Lett.* **1988**, *89*, 35–47. [CrossRef]
23. Elderfield, H.; Upstill-Goddard, R.; Sholkovitz, E.R. The rare earth elements in rivers, estuaries, and coastal seas and their significance to the composition of ocean waters. *Geochim. Cosmochim. Acta* **1990**, *54*, 971–991. [CrossRef]
24. Sharma, A.; Rajamani, V. Weathering of gneissic rocks in the upper reaches ofCauvery River, South India: Implications to neo-tectonics of the region. *Chem. Geol.* **2000**, *166*, 203–223. [CrossRef]
25. Yang, S.Y.; Jung, H.S.; Choi, M.S.; Li, C.X. The rare earth element compositions of the Changjiang (Yangtze) and Huanghe (Yellow) river sediments. *Earth Planet. Sci. Lett.* **2002**, *201*, 407–419. [CrossRef]
26. Shynu, R.; Rao, V.P.; Kessarkar, P.M.; Rao, T.G. Rare earth elements in suspended and bottom sediments of the Mandovi estuary, central west coast of India: Influence of mining. *Estuar. Coast. Shelf Sci.* **2011**, *94*, 355–368. [CrossRef]
27. Cavalcante, F.; Belviso, C.; Piccarreta, G.; Fiore, S. Grain-size control on the rare earth elements distribution in the late diagenesis of Cretaceous shales from the southern Apennines (Italy). *J. Chem.* **2014**, *2014*, 841747. [CrossRef]
28. Su, N.; Yang, S.; Guo, Y.; Yue, W.; Wang, K.; Yin, P.; Huang, K. Revisit of REE fractionation during chemical weathering and river sediment transport. *Geochem. Geophys. Geosyst.* **2017**, *18*, 935–955. [CrossRef]
29. Babu, S.S.; Ramana, R.V.; Rao, V.P.; Ram Mohan, M.; Sawant, S.; Satyasree, N.; Keshav Krishna, A. Rare earth elements of sediments in rivers and estuaries of the east coast of India. *Curr. Sci.* **2021**, *120*, 519–537. [CrossRef]
30. Babu, S.S.; Rao, V.P.; Rammohan, M. Controls on the distribution and fractionation of rare earth elements in recent sediments from the rivers along the west coast of India. *Environ. Earth Sci.* **2024**, *83*, 547. [CrossRef]
31. Gromet, L.P.; Dymek, R.F.; Haskin, L.A.; Korotev, R.L. The "North American shale composite": Its compilation, major and trace element characteristics. *Geochim. Cosmochim. Acta* **1984**, *48*, 2469–2482. [CrossRef]
32. Haskin, L.A.; Haskin, M.A. Rare earths in European shales: A redetermination. *Science* **1966**, *154*, 507–509. [CrossRef]
33. Kamber, B.S.; Greig, A.; Collerson, K.D. A new estimate for the composition of weathered young upper continental crust from alluvial sediments, Queensland, Australia. *Geochim. Cosmochim. Acta* **2005**, *69*, 1041–1058. [CrossRef]
34. Gao, S.; Luo, T.C.; Zhang, B.R.; Zhang, H.F.; Han, Y.W.; Hu, Y.K.; Zhao, Z.D. Chemical composition of the continental crust as revealed by studies in East China. *Geochim. Cosmochim. Acta* **1998**, *62*, 1959–1975. [CrossRef]

35. Viers, J.; Dupré, B.; Gaillardet, J. Chemical composition of suspended sediments in World Rivers: New insights from a new database. *Sci. Total Environ.* **2009**, *407*, 853–868. [CrossRef] [PubMed]
36. Bayon, G.; Toucanne, S.; Skonieczny, C.; André, L.; Bermell, S.; Cheron, S.; Dennielou, B.; Etoubleau, J.; Freslon, N.; Gauchery, T.; et al. Rare earth elements and neodymium isotopes in world river sediments revisited. *Geochim. Cosmochim. Acta* **2015**, *170*, 17–38. [CrossRef]
37. Cullers, R.L.; Chaudhury, S.; Kilbane, N.; Koch, R. Rare earths in size fractions and sedimentary rocks of Pennysylvanian-Permian age from the mid-continent of the USA. *Geochim. Cosmochim. Acta* **1979**, *43*, 1285–1301. [CrossRef]
38. McLennan, S.M. Relationships between the trace element composition of sedimentary rocks and upper continental crust. *Geochem. Geophys. Geosyst.* **2001**, *2*, 2000GC000109. [CrossRef]
39. Condie, K.C. *Earth as an Evolving Planetary System*; Elsevier Academic Press: Amsterdam, The Netherlands, 2005; 447p.
40. Babu, S.S.; Ramana, R.V.; Rao, V.P.; Ram Mohan, M.; Satyasree, N. Mineralogy and geochemistry of the sediments in rivers along the east coast of India: Inferences on weathering and provenance. *J. Earth Syst. Sci.* **2021**, *130*, 60. [CrossRef]
41. Babu, S.S.; Ramana, R.V.; Rao, V.P.; Ram Mohan, M.; Krishna, A.K.; Sawant, S.; Satyasree, N. Composition of the Peninsular India Rivers Average Clay (PIRAC): A reference sediment composition for the upper crust from Peninsular India. *J. Earth Syst. Sci.* **2020**, *129*, 39. [CrossRef]
42. Singh, P.; Rajamani, V. REE geochemistry of recent clastic sediments from the Kaveri Flood plains, southern India: Implication to source area weathering and sedimentary processes. *Geochim. Cosmochim. Acta* **2001**, *65*, 3093–3108. [CrossRef]
43. Sensarma, S.; Rajamani, V.; Tripathi, J.K. Petrography and geochemical characteristics of the sediments of the small River Hemavati, southern India: Implications for provenance and weathering processes. *Sediment. Geol.* **2008**, *205*, 111–125. [CrossRef]
44. Rajamani, V.; Tripathi, J.K.; Malviya, V.P. Weathering of lower crustal rocks in the Kaveri River catchment, southern India: Implications to sediment geochemistry. *Chem. Geol.* **2009**, *265*, 410–419. [CrossRef]
45. Sharma, A.; Sensarma, S.; Kumar, K.; Khanna, P.P.; Saini, N.K. Mineralogy and geochemistry of the Mahi River sediments in tectonically active western India: Implications for Deccan large igneous province source, weathering and mobility of elements in a semi-arid climate. *Geochim. Cosmochim. Acta* **2013**, *104*, 63–83. [CrossRef]
46. Babu, S.S.; Prajith, A.; Rao, V.P.; Rammohan, M.; Ramana, R.V.; Satyasree, N.S. Composition of river sediments from Kerala, southwest India: Inferences on lateritic weathering. *J. Earth Syst. Sci.* **2023**, *132*, 150. [CrossRef]
47. Babu, S.S.; Prajith, A.; Rao, V.P.; Rammohan, M.; Ramana, R.V.; Satyasree, N. Sources of rare earths and prospects for a viable REE deposit in river sediments of Kerala, Southwest India. *Curr. Sci.* **2024**, *126*, 345–359. [CrossRef]
48. Babu, S.S.; Purnachandra Rao, V.; Mohan, M.R. Clay Mineralogy and Major and Trace Element Geochemistry of Recent Sediments in Rivers Along the West Coast of India: Implications for Provenance and Chemical Weathering. *Minerals* **2025**, *15*, 43. [CrossRef]
49. GSI. Geological Map of India. In *Geological Survey of India*, 7th ed.; GSI: Bangalore, India, 1998.
50. Krishnan, M.S. *Geology of India and Burma*, 6th ed.; CBS Publishers: Delhi, India, 1982.
51. Ramesh, R.; Subramanian, V.; Van Grieken, R.; Van't Dack, L. The elemental chemistry of sediments in the Krishna River basin, India. *Chem. Geol.* **1989**, *74*, 331–341. [CrossRef]
52. Subramanian, V. The sediment load of Indian rivers. An update. In *Erosion and Sediment Yield: Global and Regional Perspectives*; Walling, D.E., Webb, B.W., Eds.; IAHS Publication No. 236; International Association of Hydrological Sciences (IAHS): Wallingford, UK, 1996; pp. 183–190.
53. Ray, S.B.; Mohanti, M.; Somayajulu, B.L.K. Suspended matter, major cations and dissolved silicon in the estuarine waters of the Mahanadi River, India. *J. Hydrol.* **1984**, *69*, 183–196. [CrossRef]
54. Dash, N.; Nayak, B.; Mohapatra, B.K. The supergene Mn-minerals in Gangpur Group, Eastern India and their genesis. *J. Geol. Soc. India* **2020**, *96*, 337–348. [CrossRef]
55. Bhattacharya, S.; Chaudhary, A.K.; Basei, M. Original nature and source of khondalites in the Eastern Ghats Province, India. In *Palaeoproterozoic of India*; Mazumder, R., Saha, D., Eds.; Geological Society, London, Special Publications; Geological Society of London: London, UK, 2012; Volume 365, pp. 147–159.
56. Folk, R.L. *Petrology of Sedimentary Rocks*; Hemphils Pub. Co.: Austin, TX, USA, 1968; p. 170.
57. Nesbitt, H.W.; Young, G.M. Prediction of some weathering trends of plutonic and volcanic rocks based on thermodynamic and kinetic considerations. *Geochim. Cosmochim. Acta* **1984**, *48*, 1523–1534. [CrossRef]
58. Nesbitt, H.W.; Young, G.M. Early Proterozoic climates and plate motions inferred from major element chemistry of lutites. *Nature* **1982**, *299*, 715–717. [CrossRef]
59. Fedo, C.M.; Nesbitt, H.W.; Young, G.M. Unravelling the effects of potassium metasomatism in sedimentary rocks and paleosols, with implications for paleoweathering conditions and provenance. *Geology* **1995**, *23*, 921–924.
60. Fedo, C.M.; Eriksson, K.A.; Krogstad, E.J. Geochemistry of shales from the Archaean (~3.0 Ga) Buhwa Greenstone Belt, Zimbabwe: Implications for provenance and source-area weathering. *Geochim. Cosmochim. Acta* **1996**, *60*, 1751–1763. [CrossRef]
61. Hassan, S.; Ishiga, H.; Roser, B.P.; Dozen, K.; Naka, T. Geochemistry of Permian–Triassic shales in the Salt Range, Pakistan: Implications for provenance and tectonism at the Gondwana margin. *Chem. Geol.* **1999**, *158*, 293–314. [CrossRef]

62. Hofmann, A.; Bolhar, R.; Dirks, P.; Jelsma, H. The geochemistry of Archaean shales derived from mafic volcanic sequences, Belingwe Greenstone Belt, Zimbabwe: Provenance, source area unroofing and submarine versus subaerial weathering. *Geochim. Cosmochim. Acta* **2003**, *67*, 421–440. [CrossRef]
63. Nesbitt, H.W.; Young, G.M. Formation and diagenesis of weathering profiles. *J. Geol.* **1989**, *97*, 129–147. [CrossRef]
64. Nesbitt, H.W.; Young, G.M.; McLennan, S.M.; Keays, R.R. Effects of chemical weathering and sorting on the petrogenesis of siliciclastic sediments, with implications for provenance studies. *J. Geol.* **1996**, *104*, 525–542. [CrossRef]
65. Cullers, R. The geochemistry of shales, siltstones and sandstones of Pennsylvanian–Permian age, Colorado, USA: Implications for provenance and metamorphic studies. *Lithos* **2000**, *51*, 181–203. [CrossRef]
66. Narayanaswamy, S. Geological Significance of Laterites of Kerala with Special Reference to Laterite Gold Occurrence in Nilambur Valley. In *Earth System Science and Natural Resource Management*; Ravindra Kumar, G.R., Ed.; Centre for Earth Science Studies (CESS): Thiruvananthapuram, India, 2004.
67. Zhao, J.; Zheng, Y.F. The intensity of chemical weathering: Geochemical constraints from marine detrital sediments of Triassic age in South China. *Chem. Geol.* **2015**, *391*, 111–122. [CrossRef]
68. Roddaz, M.; Viers, J.; Brusset, S.; Baby, P.; Boucayrand, C.; Hérail, G. Controls on weathering and provenance in the Amazonian foreland basin: Insights from major and trace element geochemistry of Northern Bolivian Amazon sediments. *Am. J. Sci.* **2006**, *306*, 257–289.
69. He, M.; Zheng, H.; Clift, P.D.; Tada, R.; Wu, W.; Luo, C. Geochemistry of fine-grained sediments in the Yangtze River and the implications for provenance and chemical weathering in East Asia. *Prog. Earth Planet. Sci.* **2015**, *2*, 32. [CrossRef]
70. Konhauser, K.O.; Powell, M.A.; Fyfe, W.S.; Longstaffe, F.J.; Tripathy, S. Trace element chemistry of major rivers in Orissa State, India. *Environ. Geol.* **1997**, *29*, 132–141. [CrossRef]
71. Moriyama, T.; Panigrahi, M.K.; Pandit, D.; Watanabe, Y. Rare earth element enrichment in Late Archean manganese deposits from the Iron Ore Group, East India. *Resour. Geol.* **2008**, *58*, 402–413. [CrossRef]
72. Giri, S.; Singh, A.K.; Tewary, B.K. Source and distribution of metals in bed sediments of the Subarnarekha River, India. *Environ. Earth Sci.* **2013**, *70*, 3381–3392. [CrossRef]
73. Viers, J.; Dupré, B.; Raun, J.J.; Deberdt, S.; Angeletti, B.; Ngoupa, J.N.; Michard, A. Major and trace element abundances, and strontium isotopes in the Nyong basin rivers (Cameroon): Constraints on chemical weathering processes and elements transport mechanisms in humid tropical environments. *Chem. Geol.* **2000**, *169*, 211–241. [CrossRef]
74. Abedini, A.; Calagari, A.A.; Mikaeili, K. Geochemical characteristics of laterites: The Ailibaltalu Deposit. *Iran. Bull. Miner. Res. Explor.* **2014**, *148*, 69–84. [CrossRef]
75. Nesbitt, H.W.; Markovics, G. Weathering of granodioritic crust, long-term storage of elements in weathering profiles, and petrogenesis of siliciclastic sediments. *Geochim. Cosmochim. Acta* **1997**, *61*, 1653–1670. [CrossRef]
76. Hannigan, R.E.; Sholkovitz, E.R. The development of middle rare earth element enrichments in freshwaters: Weathering of phosphate minerals. *Chem. Geol.* **2001**, *175*, 495–508. [CrossRef]
77. Braun, J.J.; Pagel, M.; Herbillon, A.; Rosin, C. Mobilization and redistribution of REEs and thorium in a syenitic lateritic profile: A mass balance study. *Geochim. Cosmochim. Acta* **1993**, *57*, 4419–4434. [CrossRef]
78. Pracejus, B.; Bolton, B.R.; Frakes, L.A.; Abbott, M. Rare-earth element geochemistry of supergene manganese deposits from Groote Eylandt, Northern Territory, Australia. *Ore Geol. Rev.* **1990**, *5*, 293–314. [CrossRef]
79. Singh, V.K.; Sahoo, R.K. Occurrence of manganese mineralization in Rayavalasa and Tudi villages of Eastern Ghat Mobile Belts, Andhra Pradesh. *Int. J. Res. Publ. Rev.* **2022**, *3*, 2924–2933. [CrossRef]
80. Ross, G.R.; Guevara, S.R.; Arribére, M.A. Rare earth geochemistry in sediments of the Upper Manso River Basin, Río Negro, Argentina. *Earth Planet. Sci. Lett.* **1995**, *133*, 47–57. [CrossRef]
81. Bhatia, M.R. Plate tectonics and geochemical composition of sandstones. *J. Geol.* **1983**, *91*, 611–627. [CrossRef]
82. Cullers, R.L. The controls on the major and trace element variation of shales, siltstones, and sandstones of Pennsylvanian-Permian age from uplifted continental blocks in Colorado to platform sediment in Kansas, USA. *Geochim. Cosmochim. Acta* **1994**, *58*, 4955–4972. [CrossRef]
83. Roser, B.P.; Korsch, R.J. Provenance signatures of sandstone-mudstone suites determined using discriminant function analysis of major-element data. *Chem. Geol.* **1988**, *67*, 119–139. [CrossRef]
84. Bhatia, M.R.; Crook, K.A.W. Trace element characteristics of graywackes and tectonic setting discrimination of sedimentary basins. *Contrib. Mineral. Petrol.* **1986**, *92*, 181–193. [CrossRef]
85. Bracciali, L.; Marroni, M.; Pandol, B.L.; Rocchi, S.; Arribas, J.; Critelli, S.; Johnsson, M.J. Geochemistry and petrography ofWestern Tethys Cretaceous sedimentary covers (Corsica and Northern Apennines): From source areas to configuration of margins. *Geol. Soc. Am. Spec. Pap.* **2007**, *420*, 73–93.
86. Balasubramaniam, K.S.; Surendra, M.; Kumar, T.V. Genesis of certain bauxite profiles from India. *Chem. Geol.* **1987**, *60*, 227–235. [CrossRef]

87. Gurumurthy, G.P. Geochemical split among the suspended and mud sediments in the Nethravati River: Insights to compositional similarity of Peninsular gneiss and the Deccan Basalt Derived sediments, and its implications on tracing the provenance in the Indian Ocean. *Geochem. Geophys. Geosystems* **2024**, *25*, e2024GC011642. [CrossRef]
88. Bhatia, M.R. Rare earth element geochemistry of Australian Paleozoic graywackes and mudrocks: Provenance and tectonic control. *Sediment. Geol.* **1985**, *45*, 97–113. [CrossRef]
89. Veizer, J.; Mackenzie, F.T. Evolution of sedimentary rocks. In *Treatise on Geochemistry*; Mackenzie, F.T., Ed.; Elsevier: Amsterdam, The Netherlands, 2014; Volume 9, pp. 399–435.
90. Bayon, G.; Freslon, N.; Germain, Y.; Bindeman, I.N.; Trinquier, A.; Barrat, J.A. A global survey of radiogenic strontium isotopes in river sediments. *Chem. Geol.* **2021**, *559*, 119958. [CrossRef]
91. Rao, V.P.; Rahaman, W.; Babu, S.S.; Ram Mohan, M. Controls of lithology, weathering, and sediment sorting on the Sr–Nd isotopic composition of river bed sediments along the east coast of India. *J. Earth Syst. Sci.* **2026**.
92. Ahmad, S.M.; Padmakumari, V.; Babu, G.A. Strontium and neodymium isotopic compositions in sediments from Godavari, Krishna and Pennar rivers. *Curr. Sci.* **2009**, *97*, 1766–1769.
93. Kessarkar, P.M.; Rao, V.P.; Ahmad, S.M.; Babu, G.A. Clay minerals and Sr–Nd isotopes of sediments along the western margin of India and their implication for sediment provenance. *Mar. Geol.* **2003**, *202*, 55–69. [CrossRef]

Disclaimer/Publisher's Note: The statements, opinions and data contained in all publications are solely those of the individual author(s) and contributor(s) and not of MDPI and/or the editor(s). MDPI and/or the editor(s) disclaim responsibility for any injury to people or property resulting from any ideas, methods, instructions or products referred to in the content.